

POLITECNICO DI TORINO

Department of Environment Land and Infrastructure

Master of Science

In Petroleum Engineering

Master Thesis



By

Chinara Babayeva

Supervised by:

Prof. Stefano Lo Russo

April-2019

ACKNOWLEDGEMENTS

I would like to thank my thesis adviser Professor Lo Russo for giving me an opportunity and encouragement to explore all the different subjects to involve in the thesis work and helping me out with many different issues during the process.

Special thanks to a Senior Geologist Elvin Ahmadov in the State Oil Company of Azerbaijan Republic (SOCAR) who provided the data for the calculations and his advice on specific points during the research.

Finally, I would like to express my profound gratitude to Politecnico Di Torino and all professors from Environment Land and Infrastructure Department.

Dedication

I dedicate this thesis to my beloved family, my mother Afet Babayeva, grandma Amina Babayeva and to my father David B. Rochford who supported and encouraged me during this course and not only.

Abstract

The Risk and Uncertainty Assessment of Geological Parameters while Estimating Oil and Gas Reserves.

One of the important aspects of the hydrocarbon reserves estimation in the petroleum industry is the uncertainties related to the geological parameters that arise due to various errors have been made such as incomplete or insufficient measurement data. According to several studies in the industry, the methods such as deterministic and stochastic are adopted.

In this research the focus was made on deterministic method with the help of the Oracle Crystal Ball software that uses the Monte Carlo simulation identify the uncertainties of the geological parameters and their affect on the reserves' estimation. The provided geological data from the State Oil Company of Azerbaijan Republic (SOCAR) helped to achieve this goal. In order to attain the determination of the uncertainties, the sensitivity charts demonstrate (in percentiles) the highest impacts of the different geological parameters have been analysed for various bed layers. Therefore, knowing these uncertainties allows engineers to manage them better and plan for the worst-case scenarios related to the reserves estimation. Under study of the thesis was the shallow depth "Guneshli" offshore field which is in the south east of Baku on the Apsheron Ridge of the South Caspian Basin, Azerbaijan. The shallow depth "Guneshli" field itself is divided into the isolated blocks I, II, III, IV, IV, V, VII, VIII, IX and X and the Monte Carlo simulation was made for the various layers A, B, C, D, E, F, G and H within these blocks which are named with an alphabetic order due to the SOCAR company's privacy policy. The comparison between results of Mball software that have been used by SOCAR and Oracle Crystal Ball that is applied in this research to define the oil and gas reserves' probabilities (P10, P50 and P90) in the Monte Carlo Distribution (Figures 16-19).

Another aspect is mentioned in the thesis work related to the definition of the transmissibility of tectonic faults between blocks of the shallow depth Guneshli offshore field that has already been undergone 3D and 2D Geological Modelling. A recently new and not commonly used method is used to build a Hierarchical tree with the help of JMP that is indeed a software used by data analysts. The data considered was geological data of each block and with simulation the similarity and grouping between them has been discovered and demonstrated with the dendrogram of Hierarchical tree (Figure 14)

| | |
|--|----|
| Table of Contents | |
| List of figures | |
| List of tables | |
| Abstract | |
| Chapter 1: Introduction | 1 |
| 1.1 Introduction, Background and Location | 1 |
| 1.2 Geological description of shallow depth “Guneshli” offshore field | 2 |
| 1.3 Aims and Objectives | 4 |
| Chapter 2: Literature Review | 5 |
| 2.1. Previous Works | 5 |
| 2.2 Cluster Analysis method | 9 |
| 2.3. Forecasting | 11 |
| 2.4. Monte Carlo method | 11 |
| 2.5. Sensitivity analysis | 14 |
| 2.7. Risk Analysis | 12 |
| 2.8. Oracle Crystal Ball software | 12 |
| Chapter 3: Methodology used and the results | 18 |
| 3.1. Application of Cluster Analysis | 18 |
| 3.2. Normalization of the data for Clustering | 18 |
| 3.3. Results of the clustering | 20 |
| 3.4. Calculation of Oil and Gas reserves | 21 |
| 3.5. Monte Carlo Simulation of the Calculated OIP with Crystal Ball Software | 25 |
| Chapter 4: Conclusions | 34 |
| REFERENCES | |

List of Figures

| | |
|--|----|
| Fig. 1 Location of structures on the Apsheron Threshold (Leonid A. Buryakovsky 2001)..... | 1 |
| Fig. 2 Monte Carlo Distribution (F.V. Rahimov 2017)..... | 6 |
| Fig. 3 Tornado Plot (F.V. Rahimov 2017)..... | 6 |
| Fig. 4 Sensitivity graph (F.V. Rahimov 2017)..... | 7 |
| Fig. 5 Risk Matrix (F.V. Rahimov 2017)..... | 7 |
| Fig. 6 Base Case Scenario (Auwalu Inuwa Mohammed 2018)..... | 8 |
| Fig. 7 Experimental Case Scenario (Auwalu Inuwa Mohammed 2018)..... | 8 |
| Fig. 8 Dendrogram of the Cluster Analysis (Hierarchical Clustering / Dendograms s.d.)..... | 10 |
| Fig. 9 The distribution of each cell (Niels Jacob Haaning Andersen 2008)..... | 15 |
| Fig. 10 Normal distribution (Niels Jacob Haaning Andersen 2008)..... | 16 |
| Fig. 11 Monte Carlo distribution (Niels Jacob Haaning Andersen 2008)..... | 16 |
| Fig. 12 The clusters of the blocks..... | 20 |
| Fig. 13 The 3D Model of the shallow depth “Guneshli” offshore field (OĞLU 2016)..... | 21 |
| Fig. 14 The 2D Model of the shallow depth “Guneshli” field (OĞLU 2016)..... | 17 |
| Fig. 15 Monte Carlo distribution of oil reserves (M ton) in terms of P90, P50, P10..... | 26 |
| Fig. 16 Monte Carlo distribution of oil reserves (MM bbl) in terms of P90, P50, P10..... | 27 |
| Fig. 17 Monte Carlo distribution of gas reserves (MM m ³) in terms of P90, P50, P10..... | 29 |
| Fig. 18 Monte Carlo distribution of gas reserves (Bcf) in terms of P90, P50, P10..... | 30 |
| Fig. 19 Tornado chart of Oil Reserves..... | 23 |
| Fig. 20 Tornado chart of Gas reserves..... | 35 |
| Fig. 21 Sensitivity charts of Oil and Gas reserves..... | 37 |

List of tables

| | |
|---|----|
| Table 1. Source and Accuracy of Volumetric Reserves Parameters (Robert H. 2001)..... | 13 |
| Table 2. The geological parameters of the blocks..... | 19 |
| Table 3. The geological parameters of the blocks after normalization..... | 20 |
| Table 4. The volumetric data for the block A..... | 22 |
| Table 5. The volumetric data for the block B..... | 22 |
| Table 6. The volumetric data for the block C..... | 23 |
| Table 7. The volumetric data for the block D..... | 23 |
| Table 8. The volumetric data for the block E..... | 23 |
| Table 9. The volumetric data for the block F..... | 23 |
| Table 10. The volumetric data for the block G..... | 24 |
| Table 11. The volumetric data for the block H..... | 24 |
| Table 12. Calculated the Oil and Gas Reserves for each block..... | 24 |
| Table 13. The total oil reserves..... | 25 |
| Table 14. The total gas reserves..... | 25 |
| Table 15. The Forecast values of the Monte Carlo simulation..... | 26 |
| Table 16. The vary of results of the Monte Carlo simulation of oil reserves (M ton) forecast (in percentiles) | 27 |
| Table 17. The Forecast values of the Monte Carlo simulation..... | 28 |
| Table 18. The vary of results of the Monte Carlo simulation of oil reserves (MM bbl) forecast (in percentiles)..... | 28 |
| Table 19. The Forecast values of the Monte Carlo simulation..... | 29 |
| Table 20. The vary of results of the Monte Carlo simulation of gas reserves (m3) forecast (in percentiles)..... | 30 |
| Table 21. The vary of results of the Monte Carlo simulation of gas reserves (Bcf) forecast (in percentiles)..... | 31 |
| Table 22. The comparison of the Monte Carlo simulation between software Crystal Ball and Mball..... | 31 |
| Table 23. Uncertain variables present in the Tornado chart..... | 33 |
| Table 24. Uncertain variables present in the Tornado chart..... | 33 |

Nomenclature

A: Area, m^2

h: Effective thickness, m

S_w : Water Saturation

ϕ : the porosity, %

B_o : Formation Volume Factor

n : is the number of observations

v : is the number of variables

x_i : is the i th observation

C_k : is the k th cluster, subset of $\{1, 2, \dots, n\}$

N_k : is the number of observations in C_k

Chapter 1

Introduction

1.1. SCB – Petroleum Geology

The Caspian Sea is a prolific hydrocarbon region with oil, gas and condensate reserves, it is surrounded by the territories of Russia, Azerbaijan, Turkmenistan and Kazakhstan. The Caspian Sea is the largest salty lake in the world and the length from north to south is 1174 km with average width 326 km, and with the total area about 375000 km². Measured depth of water in the middle and the Southern part of the Caspian Sea is approximately 788 m and 1025 m, respectively. (Leonid A. Buryakovsky 2001)

Based on the geological and geophysical investigation, there are more than forty anticlinal structures within the western part of the South Caspian Basin. (Leonid A. Buryakovsky 2001)

Starting from 1949 the offshore development has been carrying out in Azerbaijan and since then the production of oil (12MMt) and condensate, gas (11 Bm³) which is nearly half pf their recoverable reserves.

Three offshore oil- and gas-bearing zones are distinguished in the Azerbaijan section of the South Caspian Basin. Are classification comprises:

1. Western portion of Apsheron-Pre Balkhan-Anticlinal Trend
2. South Apsheron Offshore Zone
3. Baku Archipelago

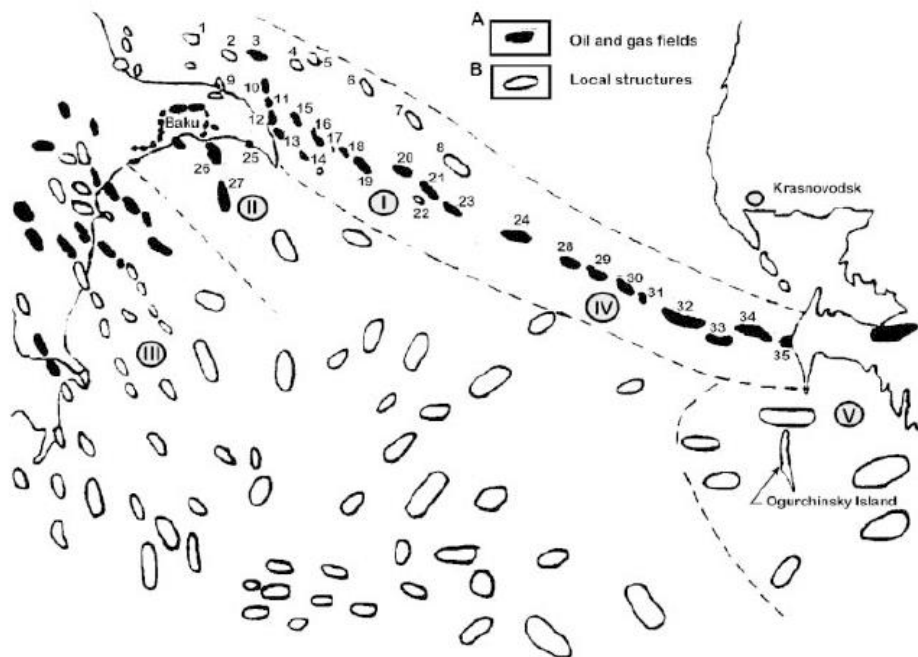


Figure 1. Location of structures on the Apsheron Threshold (Leonid A. Buryakovsky 2001)

(Modified after Bagir-zadeh et al., 1974). A—Oil and gas fields; B—prospects: 1—Goshadash, 2—Apsheeron Bank, 3—Agburun Deniz, 4—Gilavar, 5—East Gilavar, 6—Danulduzu, 7—Ashrafi, 8—Karabakh, 9—Mardakyan Deniz, 10—Darvin Bank, 11—Pirallaghi Adasi (Northern Fold), 12—Pirallaghi Adasi (Southern Fold), 13—Gyurgyan Deniz, 14—Dzhanub, 15—Khali, 16—Chalov Adasi, 17—Azi Aslanov, 18—Palchygh Pilpilasi, 19—Neft Dashlary, 20—Gyuneshli, 21—Chyragh, 22—Ushakov, 23—Azeri, 24—Kyapaz, 25—Shakh Deniz, 26—Gum Deniz, 27—Bakhar, 28—Livanov-West, 29—Livanov-Center, 30—Livanov-East, 31—Barinov, 32—Gubkin (Western, Central, Eastern), 33—Zhdanov (Western, Eastern, Pre-Cheleken Dome), 34—LAM, 35—Cheleken.

The structural traps are observed in the South Caspian Depression. The hydrocarbon accumulation can be defined on the following traps with anticlinal folds to monoclines are mainly divided into reverse faults and fractures. Many structures are interrupted by the mud diapirs and mud volcanoes. The great number of the accumulations are in Fluvial-Deltaic Middle Pliocene sediments. The size of the Mud Volcanoes varies up to 400 m and diameters of up to kilometres. (A.Narimanov s.d.)

With reference to Mud Volcanoes, their approximate age is about 2.5 million years and a number remain active today. As hasty subsidence has been ongoing the observed concentration is with a great Pliocene sedimentation rates of Mud Volcanoes. (Leonid A. Buryakovsky 2001)

1.2. About “Guneshli” Field

The “Guneshli” field is located in the southeast of Baku, 120-135 km offshore on the Apsheeron Ridge of the South Caspian Basin. The structure as mentioned before is asymmetric anticline and plays an important part in the oil production of SOCAR, Azerbaijan not only now but also in the near future.

In 1979 the discovery of the “Guneshli” field took a place by the 2nd exploration well in the area. The oil reserves are discovered X horizon of the Balakhany suite, Balakhany suite, Fasila (Pereryva) suite, Upper Kirmaky, and Lower Kirmaky and gas reserves are discovered in the VI and VII horizons of the Balakhany suite, Upper Kirmaky, Lower Kirmaky, and Kala suite. (A.A. Narimanov s.d.)

Accumulation of oil and gas is related to the anticlinal structure with the size of 12x4 km, expanding from the northwest to southeast, the type of the reservoir is layer-shielding. (V. J. Abdullayev s.d.) (14) the structure is complicated by series of longitudinal and transverse faults, that are divided into 15

tectonic with three zones: northeast(I — VI), central (VII — X) and southwest(XI — XV) . (A. A. Фейзуллаев 2018) (15) The amplitude of the layer displacement of these faults in the different sides of the structure and ranges from 20-50 m to 100 m. The reservoir distribution is controlled by tectonic features of the structure. (V. J. Abdullayev s.d.) According to the studies, dip faults generate isolated blocks which are I, II, III, IV, IV, V, VII, VIII, IX and X. (A.A. Narimanov s.d.)

The research and exploration works revealed that the horizons II, III of the Surakhani layer, the horizon IV of the Sabunchi layer and the horizons V, VI of the Balakhani layer are consisted of the gas-condensate. And the horizons VII, VIII, IX, X of the Balakhani layer, the layers FLD, and QUG are consisted of the oil as the layers QUQ, QA are consisted of the oil-condensate. (B.Ə. 2015, 20)

This structure was discovered in the result of seismic analysis in 1958-1963. The deep drilling has started from 1977 from the well 4 in the horizon X Blakhany with flow rate of 230 ton/day in the depth of 3455-3423 m. The observation from analysis was that the horizons 4, 5 and 6 contained gas condensate and the horizons 8,9,10 contained oil. (V. J. Abdullayev s.d.).

At present, SOCAR's essential production zone is the Fasial Suite and the X horizon of the Balakhany suite. The focus of this thesis is with reference to the X horizon of the Balakhany suite and the following I, II, III, IV, IV, V, VII, VIII horizons where the Cluster Analysis has been applied in order to discover the similarities between those blocks and define if they are transmissible or not.

At this moment the main oil and gas production of the State Oil Company of Azerbaijan Republic (SOCAR) is currently 83% from the "Guneshli" and the "Neft Dashlari" beds.

The goal of my work is to define residual reserves of the "Guneshli" field and Risk Assessment of the properties affection the residual reserves.

The current activities held by the State Oil Company of the Azerbaijan Republic (SOCAR) are the exploration of oil and gas fields, production, process and transport of oil, gas and gas condensate, marketing petroleum and petrochemical products as in domestic and also international markets. The petroleum activities take place in many countries such as Georgia, Turkey, Romania, Switzerland, Germany, Italy and Ukraine. (SOCAR s.d.)

1.3. Aims and Objectives

The impact of the geologic parameters on the oil and gas reserves estimation and following risk assessment is investigated as the aim of this project. Using Monte Carlo simulation with the help of the Oracle Crystal Ball software the Tornado and Sensitivity charts will be built and analysed and the comparison between “Mball” software used previously by SOCAR and “Oracle Crystal Ball” software used for this research will be discussed.

The secondary objective of the thesis is focused on the Hierarchical Cluster Analysis of the geological parameters of the shallow water “Guneshli” field in order to prove the transmissibility between the faults of the various blocks existing in the system. Reaching out the JMP software which is mainly used in the field of the statistical data that groups the data with the similarity of the updated data and builds a dendrogram where the clustering is conducted.

The analysis in this project will be achieved with the help of:

1. Various literature reviews
2. Geological data provided by “SOCAR”
3. The use of the Oracle Crystal Ball software, Monte Carlo Simulation
4. The use of the JMP software
5. Hierarchical Clustering and dendrograms

The results of the simulation with the Oracle Crystal Ball will be discussed in the sensitivity charts where critical geological parameters will be discussed. The Hierarchical Clustering will be concluded with the dendrograms and discussion of the results.

Chapter 2

Literature Review

2.1. Previous Works

The Estimation of the Oil and Gas Reserves has always been a significant economic hurdle that is highlighted in scientific papers and companies' investigation in the potential development of projects. Basic knowledge of the Risk and Uncertainty Assessment during the Estimation of the Oil and Gas plays an important role in terms of the development phase of the ongoing or planned projects. There are several scientific papers and dissertations on the mentioned subject.

Furthermore, the PhD Dissertation work of Elvin Ahmadov (Senior Geologist in SOCAR) was based on the Risk Assessment of the "Guneshli" and "Neft Dashlari" fields in South Caspian Basin, Azerbaijan. In his work the focus related to 3D Modelling of "Guneshli" and "Neft Dashlari" field, structural and tectonic analysis applying Cluster Method on the geologic parameters to define if the tectonic faults are transmissible or not, the estimation of the hydrocarbon reserves with the Monte Carlo Simulation and the Risk Assessment of the Estimated Reserves.

In order to determine the nature of the tectonic faults, the study of the geological-geophysical and mining parameters with the help of Cluster Analysis has been made. Further, with the use of deterministic models, the residual reserves of "Guneshli" and "Neft Dashlari" fields has been determined with the dynamic simulation (The monte Carlo Method) and with the sensitivity analysis the Tornado chart has also been made as an outcome. To determine the reliability of the calculated reserves, the geological risk assessment has been made based on the geological-geophysical parameters. (OĞLU 2016, 5-6)

One of the recent works related to the estimation of the resaves considering uncertainty and risk assessments has been done by F.V. Rahimov, A.Sh. Eminov and R.M. Huseynov at the SPE Annual Caspian Technical Conference and Exhibition in Baku, Azerbaijan in 2017. According to the research, the Monte-Carlo techniques has been applied to analyse the evaluation of different critical geological parameters from the initial values in order to estimate distribution within P10, P50 and P90 probability curve where the distribution of the volumetric hydrocarbon reserves.

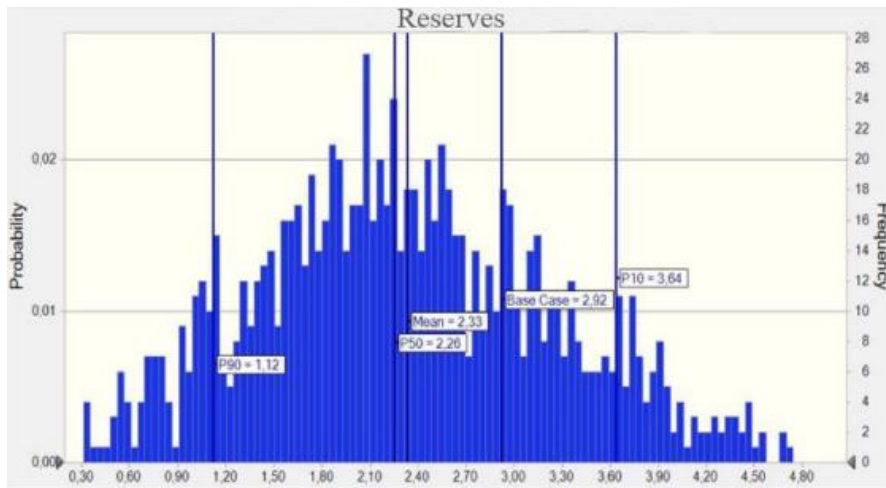


Figure 2. Monte Carlo Distribution (F.V. Rahimov 2017)

The following Tornado and Sensitivity graph have demonstrated, where the affect of the several parameters on the reserves' estimation is plotted in terms of the percentage:

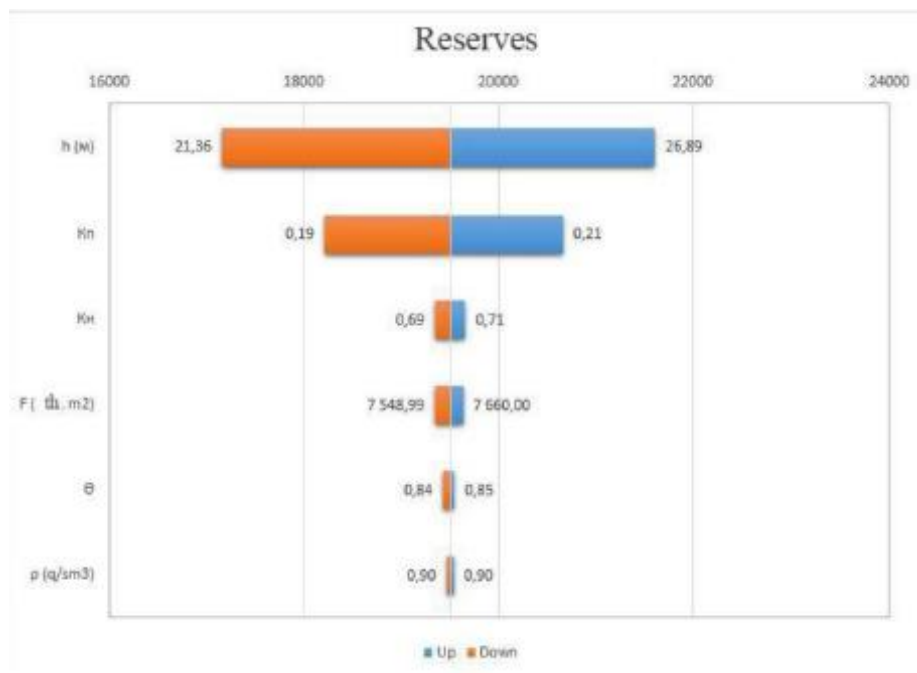


Figure 3. Tornado Plot (F.V. Rahimov 2017)

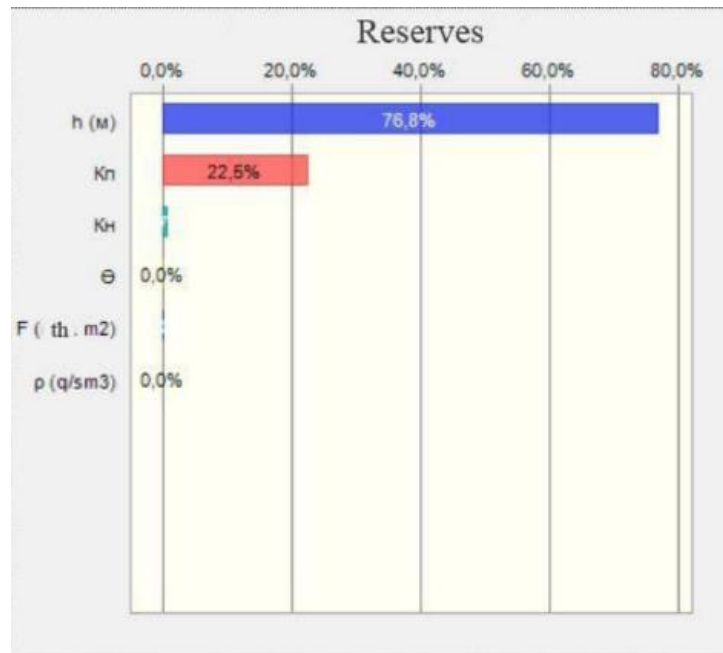


Figure 4. Sensitivity graph (F.V. Rahimov 2017)

The research is also taking into the consideration the risks in terms of the parameters and reflected in the Risk Matrix where the consequences and likelihood are divided into High, Medium and Low levels.

From the matrix the porosity results having an affect in the level High to the estimation of the hydrocarbon reserves. And the risk level of the other parameters such as Oil Saturation and Oil Density affects in a lower level of the risk compared to the Porosity. (F.V. Rahimov 2017, 1-4).

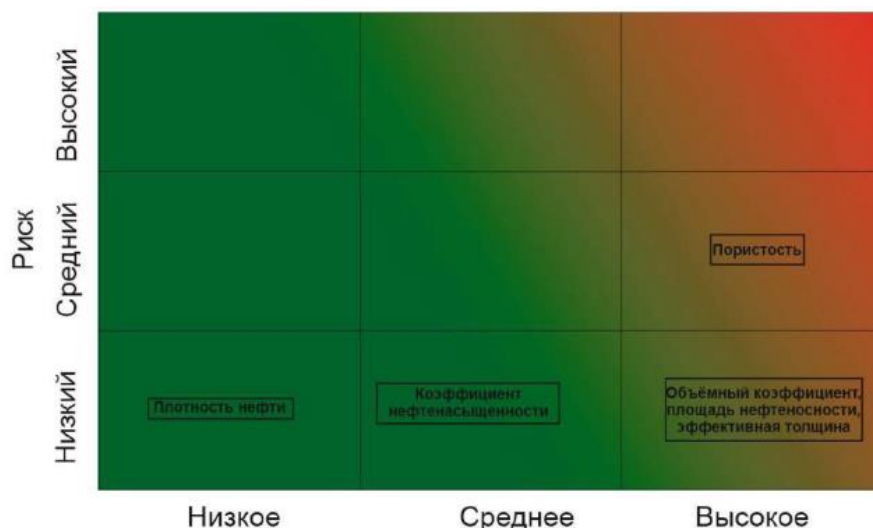


Figure 5. Risk Matrix (F.V. Rahimov 2017)

As uncertainty is a serious issue with any project managed by engineers in the phase of the reserve estimation in petroleum engineering, for example research work has been presented by Auwalu Inuwa Mohammed, Hassan Abdurahman, Sulaiman Dodo Ibrahim, and Bello Mohammed Adamu from

Abubakar Tafawa Balewa University at the Nigeria Annual International Conference and Exhibition in Lagos, Nigeria in 2018. In this paper, the undergone research evaluated the reserve estimation of the multi-layered reservoir with the help of Monte Carlo Simulation accompanied by the Oracle Crystal Ball software for sensitivity analysis of the. In this case, the scenarios for the distribution differ from the previous presented paper. The consideration of the distributions: Lognormal, Triangular, Normal, Uniform change for each the geological parameter. (Auwalu Inuwa Mohammed 2018, 4)

For instance, the number of trials in this work varied from 100 up to 2500 trials, and the optimum was selected the range of 800-1000. Their results have shown the number of various scenarios, which were the Base Case simulation and the Experimental Simulation. In the Base Case scenario, the maximum 165.85 MMSTB reserve and minimum 25.51 MMSTB of oil reserve were estimated. In the Experimental Simulation, the maximum 175.48 MMSTB reserve and minimum 27.00 MMSTB oil reserve were estimated. And respectively, the sensitivity chart was demonstrated for each case of the scenarios. (Auwalu Inuwa Mohammed 2018, 5-8). The discussed results of the Oracle Crystal Ball software analysis is shown below for the Base Case and Experimental Case scenarios:

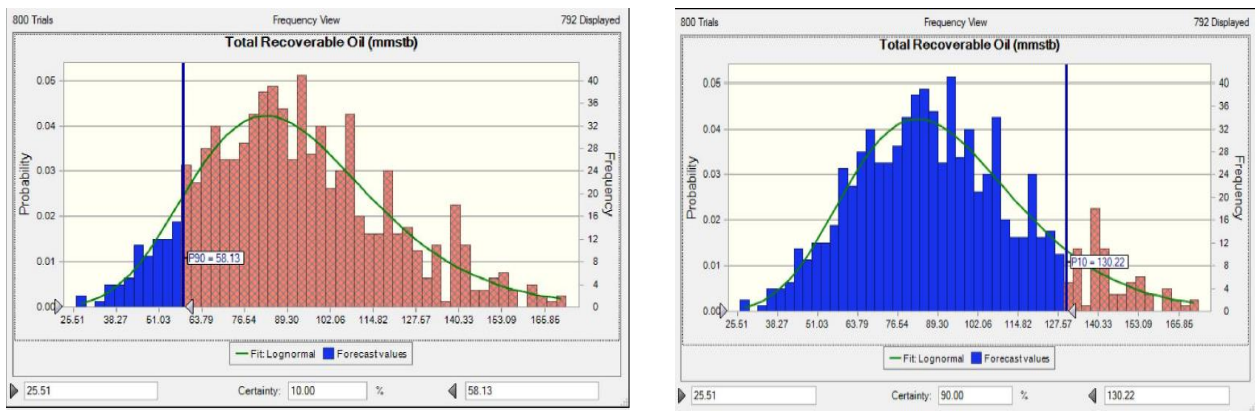


Figure 6. Base Case Scenario (Auwalu Inuwa Mohammed 2018, 6,7)

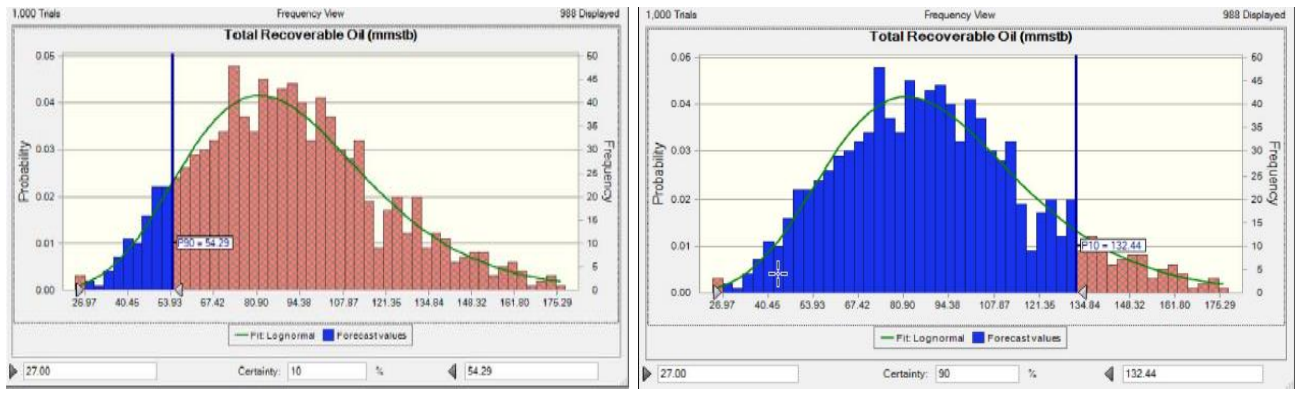


Figure 7. Experimental Case Scenario (Auwalu Inuwa Mohammed 2018, 9,10)

2.2. Cluster Analysis method

The definition of the Cluster analysis was given by Davis, John C. in his book of Statistics and Data Analysis in Geology. The description of the Cluster Analysis based on the procedure that classifies the observations into the two groups. The groups are distinguished by the assortment of homogeneous and distinct from the other groups. (Davis s.d., 487).

From the dataset, the Clustering can identify the grouping or enforce segregation. The parameters that are present can be undergone the subdivision (clustering) of the consistent groups that have the similarities between them. (Mark Baker 2015, 2)

When a large amount of information is available and at the same time the n members of parameters are ungrouped, in most of the cases the procedure of the grouping is recommended. Consequently, the members consist only several members. The initial step would be to relate the two subsets, which are united and then they will be decreased by one of the subsets until reaching the least damage of the optimal value. In order to assure the optimal value, this procedure of grouping of several n members into the groups will be applied and it can be continued until the all the n members are arranged into the groups. The result will be systematic reduction of the number of subsets which is called "hierarchical grouping". (Joe H. Ward March 1963, 238). A tree diagram named the dendrogram is shown as a tree diagram which has a cluster hierarchy. The most similar clusters are joined together and make a new sing cluster and never apart. Below shown the example of the Hierarchical Clustering where is represented the distance or the dissimilarity between clusters, remember the distance is not the physical. Here is given vertical lines that performs the objects and clusters and at the same time the horizontal lines that are split into further horizontal lines. Each horizontal line split by the vertical line gives the distance(dissimilarity) between each cluster. (Hierarchical Clustering / Dendograms s.d.)

For instance, if the numbers 6 and 13 represent Blue and Red, respectively, following the interpretation in the dendrogram the observation can be made is that, they have a much greater distance between each other. (Hierarchical Clustering / Dendograms s.d.)

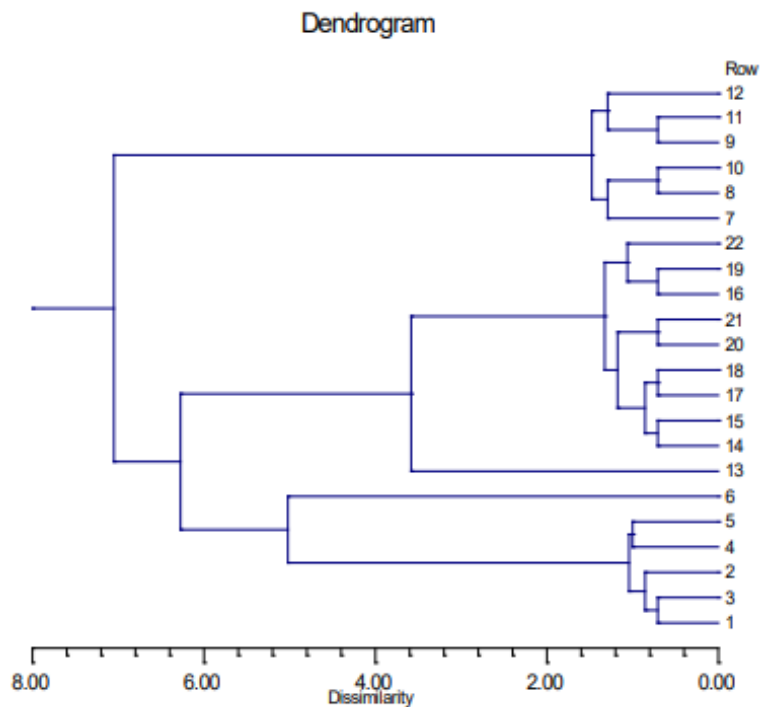


Figure 8. Dendrogram of the Cluster Analysis (Hierarchical Clustering / Dendograms s.d.)

Some geological studies require grouping analogical characteristic of the measured parameters of samples. Applying cluster analysis as a statistical mechanism, it allows the discovery of similarities between these parameters. The outcome of a comparison of the samples in sequence of the pair-by-pair is a two-dimensional hierarchical diagram on which the natural breaks are visible. (Parks 1966).

There are many types of software that can be applied to process the Hierarchical Clustering. One of them, JMP software is used to compute the statistical data. The approach starts with treating every observation as its own cluster and at each level, the two clusters that are adjacent in terms of distance are merged into a single cluster. Here when the distance is mentioned, it is not related to the geographic distance, but the multivariate space defined by entered variables of the resemblances and dissimilarities. (Surek December 2013) The dendrogram displays how the clustering is conducted, the reading starts from the left to the right. Depending on which is useful for the applicative, it is possible to pick any desired level of similarity or dissimilarity (JMP Statistical Discovery s.d.)

There are two ways to perform a cluster analysis such as R-type or Q-type.

1. R-type analysis allows to observe the variables that co-occur more regularly.
2. Q-type analysis allows to observe the similarity or dissimilarity of the samples. (Surek December 2013)

2.3. Forecasting

The underlying fundamental of the forecasting is the correlation between everything. Since there is a major complexity between everything the correlation needs expedient assumptions. In order to follow these assumptions one of the simple ways is to study the historical data within a comparably short time period. It is potentially a hazard to confuse the forecast assumption and conclusion. So, it is important to reconsider the assumptions in light of the conclusions.

The necessary steps for the forecast are the following:

1. Validation through investigation of the given data
2. To make a rational assumption
3. Control a relativity between the given data.
4. Evaluation of the results. (Burns 2018)

By means of mentioned steps, in this thesis work stochastic analysis has been applied. This method is commonly used in oil and gas industry as Monte Carlo simulation, which is a statistics-based implement that crops probability versus oil and gas reserves. (J. H. Schulze 2012, 1-4)

But before approaching this method the uncertainties of the reservoir data should be considered. Uncertainties are observed mainly from different measurement errors, inadequate data, missing data etc. (J. H. Schulze 2012)

There are several sources of uncertainties in the reservoir data, the most common ones come from field or laboratory data that have a degree of inaccuracy either related to the human error or measuring instruments. In any case, these errors can be assessed and reduced by applying an estimation method. (Auwalu Inuwa Mohammed 2018)

2.4. Monte Carlo Method

The origination of the Monte Carlo method suggests that many relationships arising in non-probabilistic contexts can be evaluated more easily by stochastic experiments than by standard analytical methods, the von Neumann – Ulam concept. The definition of Monte Carlo method can be explained as design and investigation of a stochastic model where a physical or mathematical process are simulated in a complete necessary aspect. From the point of view of computing science, analysis of Monte Carlo is based on the sequence of sampling theory and numerical analysis.

The followings are the major steps in a Monte Carlo calculation:

1. Reducing statistical data with selecting or designing a probability model.
2. Introducing odd numbers and corresponding odd variables
3. Composing and implementing variance-decreasing techniques.

Many publications suggest distinctive characteristics of the Monte Carlo method that are followed:

1. The Monte Carlo method applies probability method to discover answers to the physical issues may or may not be linked to the probability.
2. The outcomes of the Monte Carlo computations considered as an approximate with the certain assurance limits rather than a definite value.
3. However, these approximations with the certain level of confidence can be enhanced proportionally with the time and money related to the issue.
4. The Monte Carlo method is an entirely numerical character, so it needs an attentive analysis of the outcomes.
5. The results of the Monte Carlo method are numerical and should be applied selectively depending on the case study. (Stoian 1965)

Broadly, when the simulation is performed generally in order to describe a physical system, it contains analogy or mathematical models. In many cases the system can be defined as a very complex, conceivably involving processes that can be poorly understood, or there is a need of a brief analysis of the uncertainties that affect the total system that has distinct parameters or elements.

(p. Behrenbruch s.d., 3)

Every parameter, used as an input data and in the calculations, needs to be interpreted with a probability distribution that represents the primary data (frequency distribution). In the case of the Monte Carlo method the primary frequency distribution may be applied directly. It is worth to perform a sensitivity calculation/analysis of the data set that has a tendency of a specific distribution.

(p. Behrenbruch s.d., 3).

In order to define the output changes of the drawn spread of the model inputs with the great number of various models, the Monte Carlo approach is an example of the uncertainty evaluation. If the observation of the output model displays a small adjustment, the consideration from this can be that the uncertainty in the model is small. But if the observation shows that the change in the model is great, this will imply that the model is quite sensitive to the adjustments and the boost of the uncertainties is established. The outcome is presented as percentiles of the Cumulative Probability

Distribution. The Uncertainty Division is categorized in 3 main levels such as P90, P50 and P10; expressing the 90th percentile, the median and 10th percentile probability efficiency of the evaluated reserves volumes respectively. (Maureen Ani 2016)

To interpret a Probability Distribution of the input data, principally it is necessary to determine a function of the Probability Distribution of the geological and technical relationships. Usually, the probability theory can disfigure the attempt of the modelling. For this reason, it is recommended the application of the distributions such as uniform, normal and lognormal. (p. Behrenbruch s.d., 4)

(2) Considering that uncertainty evaluation is a major issue in the Oil and Gas industry, there are several views of this subject related to the reserves estimation. One of the few opinions arrives from DeSouarcy. DeSouarcy’s argument on the amount of uncertainty related to the reserve estimation is based on the techniques, and particular level of certainty associated with each parameter. The table below, sums up DeSouarcy’s data for the parameters used in a volumetric estimation of OIP. (Robert H. 2001, 3)

Table 1—Source and Accuracy of Volumetric Reserves Parameters After DeSouarcy, 1979

| FACTOR | SOURCE OF ESTIMATE | APPROXIMATE RANGE OF EXPECTED ACCURACY |
|------------------|-------------------------------|--|
| Area | Drill Holes | +/- 10-20% |
| | Geophysical Data | +/- 10-20% |
| | Regional Geology | +/- 50-80% |
| Pay Thickness | Cores | +/- 5-10% |
| | Logs | +/- 10-20% |
| | Drilling Time & Samples | +/- 20-40% |
| | Regional Geology | +/- 40-60% |
| Porosity | Cores | +/- 5-10% |
| | Logs | +/- 10-20% |
| | Production Data | +/- 10-20% |
| | Drill Cuttings | +/- 20-40% |
| | Correlations | +/- 30-50% |
| Water Saturation | Capillary Pressure Data | +/- 5-15% |
| | Oil Based Cores | +/- 5-15% |
| | Saturation Logs | +/- 10-25% |
| | Adjusted Routine Cores | +/- 25-50% |
| | Correlations | +/- 25-60% |
| FVF | PVT Analysis of Fluid Samples | +/- 5-10% |
| | Correlations | +/- 10-30% |

Table 1. Source and Accuracy of Volumetric Reserves Parameters (Robert H. 2001)

However, it is relevant to acknowledge the sources of the uncertainty before improving the accuracy of estimation of reserves. In order to do that, the division of the sources of the uncertainties is given below:

1. The inaccuracy of the measurement
2. Computation approximation

3. Lack of data
4. Stochastic Systems (Robert H. 2001, 4)

2.5. Sensitivity Analysis

By the time the final reserves distribution has been discovered, there are number of the geological parameters that affect the distribution. When the uncertainty analysis has been obtained, the ignorance of some important geological parameters may influence the results. The sensitivity analysis is implemented in the cases when the desire of a better understanding of the various parameters that affect the uncertainty analysis is needed. In order to apply this, the Tornado chart should be built to visualize the main elements that highly affect mentioned uncertainty analysis. (Arvin Khadem Samimi 2014, 335) (18) In the other words, in order to correlate the relative importance of the parameters in sensitivity analysis, the use of Tornado diagram as a special kind of the bar chart is applied. Here, the Y-axis is consisted each type of the uncertainty at base values and the X-axis is consisted in the spread or correlation of the uncertainty to the examined output. (AureaWorks- Quantitative Risk Analysis and Modeling Techniques 2016, AureaWorks s.d.)

2.6. Risk Analysis

In order to overcome the uncertainties related to geological parameters that affect the reserve estimation leading to a better decision making, the risk analysis provides a rational basis in geophysics, geology and reservoir engineering. So the necessity of the evaluation of risks related to the geological parameters with different techniques will help to achieve to understand which parameters are critically in an uncertain level. (B. Corre 2000)

2.7. Oracle Crystal Ball software

Crystal Ball is an 'Add-in' application for Microsoft Excel, this program allows the user to define assumptions for the input cells in contrast to Excel's static cells, which contains explicit values such as geological parameters in this case. The stochastic distribution of the specific values made by Crystal Ball cells that used for the Monte Carlo simulations. (Niels Jacob Haaning Andersen 2008 , 1). Simulation is used in order to fast set up and analyse many probable outcomes as Excel itself doesn't have that function to run a simulation, so add-on Crystal Ball is utilized for this activity. (Oracle 2008). The Crystal Ball application will calculate an input data of the one or more cells based on the assumptions and

statistical input and will make a prediction as an output cell, which is resulted as a “Forecast” cell. (Niels Jacob Haaning Andersen 2008).

When the Crystal Ball has been generated, it takes over the values in the cells with a random number, drawn from the specified distribution. It will automatically revise the calculations and the forecast cells be be updated with advanced input values. This cycle can be repeated several set times. Therefore, the Forecasts can be exposed in the such picture as histograms and revealing statistics like mean, standard deviations and correlations. (Niels Jacob Haaning Andersen 2008 , 2).

Each input cell that is calculated is used as an Assumption cell, that has a constant number in the cell. If it is for example, equal to 1, the application will assume it as a formula. Each parameter in the cell can be chosen for particular distribution such as Normal, Triangular, Uniform, Lognormal, Beta and BetaPERT. (Niels Jacob Haaning Andersen 2008 , 6)

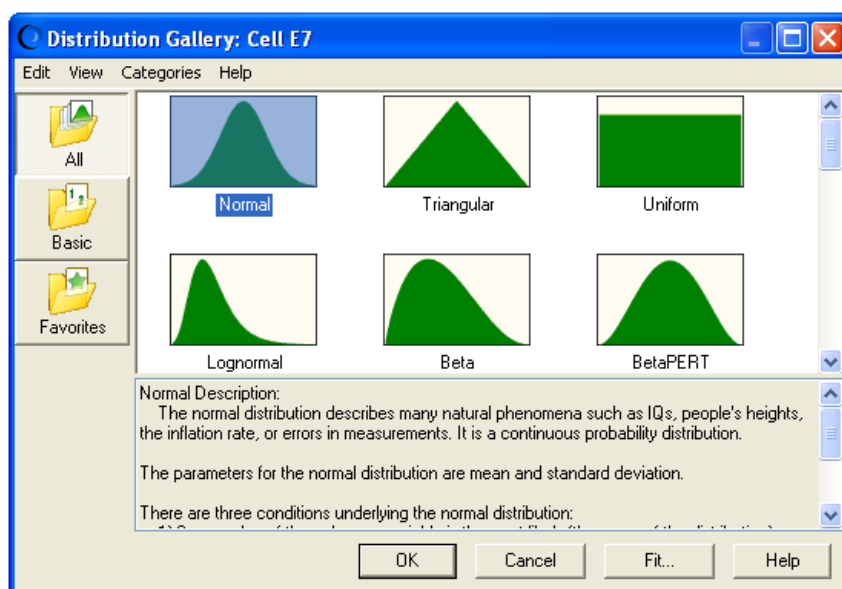


Figure 9. The distribution of each cell (Niels Jacob Haaning Andersen 2008)

After defining the distribution, further the characteristic parameters should be determined such as Mean and Std. Dev.(Figure 12) (Niels Jacob Haaning Andersen 2008 , 7)

In order to proceed to the Forecast, the data from cells that are collected is used for histograms, descriptive statistics, trend- and sensitivity charts. At the end of the simulation the forecast will be resulted with the histogram shown as an example below. (Figure 13) (Niels Jacob Haaning Andersen 2008 , 9)

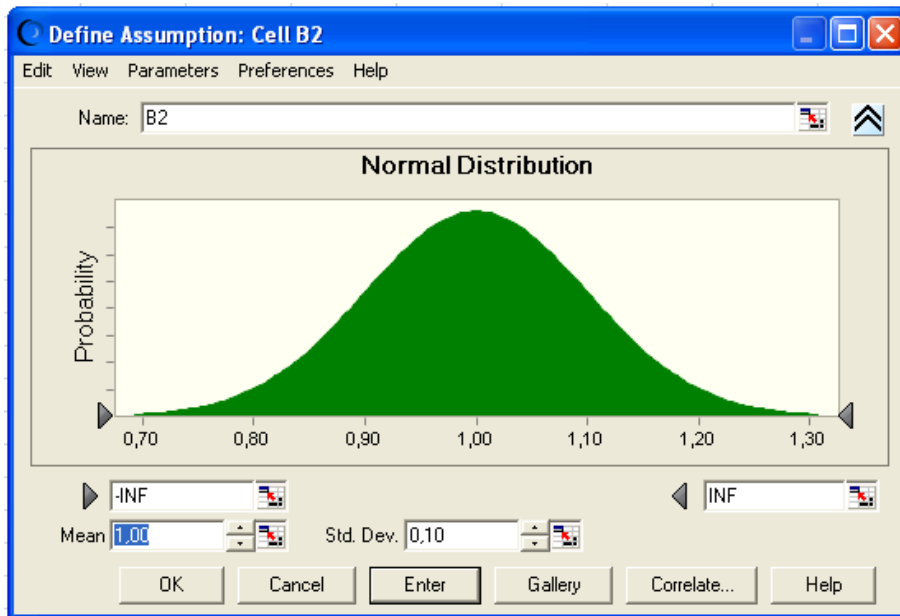


Figure 10. Normal distribution (Niels Jacob Haaning Andersen 2008)

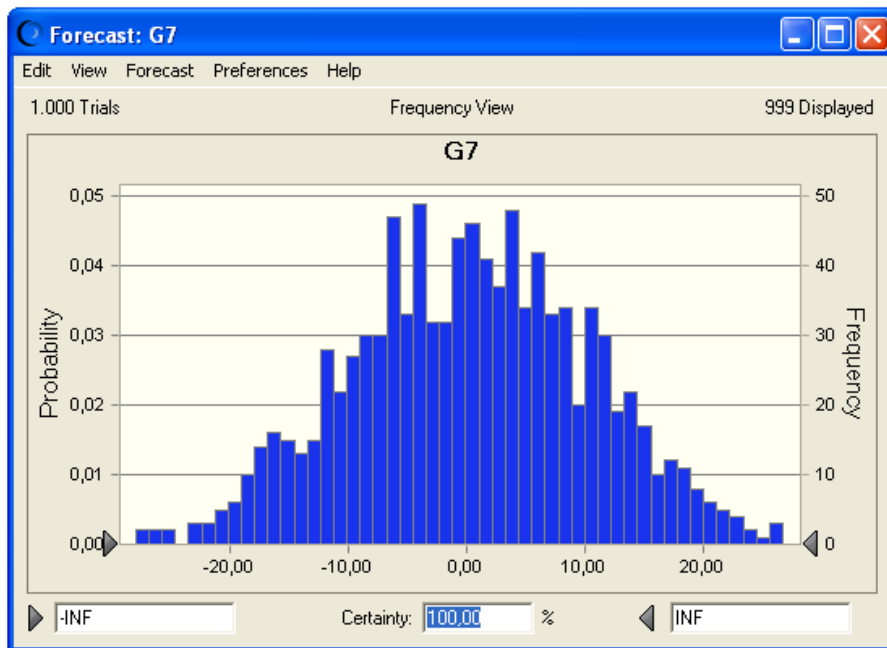


Figure 11. Monte Carlo distribution (Niels Jacob Haaning Andersen 2008)

As the Crystal Ball simulation is running, the Forecast cells will be built up for each cell that are demonstrated as a result of running software. (Niels Jacob Haaning Andersen 2008 , 10)The number for the simulation trials can be set for example 5000 and then the 5000 forecast(or possible outcomes) will be created. (Oracle 2008)

Depending on the choice of the applicant, the Sensitivity analysis can be demonstrated by the end of the simulation. The default set up can be as a percentage of the assumption chosen variables(parameters) that has a contribution to the Forecast cell. (Niels Jacob Haaning Andersen 2008 , 14)

The last built model of the Crystal Ball software is the Tornado chart, that defines which model variables are the most important in terms of the percentage that affect the uncertainty analysis assumption. (Oracle 2008)

Chapter 3

Methodology used and the results.

3.1. Clustering used to determine the transmissibility of faults.

The software JMP used in the process of the clustering provides four platforms to observe different cluster methods that are:

1. Hierarchical Cluster
2. K Means Cluster
3. Normal Mixtures
4. Latent Class Analysis

However, from these four methods the most appropriate the use of the Hierarchical Cluster analysis has been chosen as it is suitable for any Data type or Modelling type, not necessary to specify the number of clusters. This type of clustering combines rows in a hierarchical sequence that is demonstrated as a tree.

The distance option between the clusters are provided by the Distance Method Formulas that can be chosen before building the tree. The Average Linkage cluster method has been chosen in this case that is calculated by the formula given below:

$$D_{KL} = \sum_{i \in C_K} \sum_{j \in C_L} \frac{d(x_i, x_j)}{N_K N_L}$$

(JMP Statistical Discovery s.d.)

Based on the geologic parameters of the blocks and the normalisation of the properties the cluster analysis has been made.

3.2. Normalization of the data.

Before the application of the Cluster Analysis with the JMP software, the normalization of the given data was required due to the difference between the units of the geological parameters.

One of the normalization methods is the Min-Max normalization that takes into an account the conversion of the engineering units into a value between 0.0 and 1.0, the minimum and the maximum values respectively. This approach allows the use of the different units in the clustering analysis as the original

units can mislead to undesirable errors in the analysis. Below given the formula used for the normalization:

$$MM(X_{ij}) = \frac{X_{ij} - X_{\min}}{X_{\max} - X_{\min}}$$

| | Effective Thickness, m | Porosity | Permeability, mD | Oil Saturation | oil viscosity, mPa *s | oil density, g/sm3 | Average pressure of the layer, MPA |
|-------------|------------------------|----------|------------------|----------------|-----------------------|--------------------|------------------------------------|
| Block1 | 67 | 0.26 | 40 | 0.69 | 1.1 | 0.862 | 21 |
| Block2 | 63 | 0.26 | 40 | 0.69 | 1.3 | 0.865 | 21 |
| Block3 | 23 | 0.26 | 40 | 0.69 | 1.1 | 0.862 | 20 |
| Block4 | 41 | 0.26 | 40 | 0.69 | 1.2 | 0.862 | 20 |
| Block5 | 25 | 0.26 | 40 | 0.69 | 1 | 0.862 | 15 |
| Block6 | 67 | 0.29 | 40 | 0.8 | 1 | 0.862 | 24 |
| Block6a | 50 | 0.26 | 40 | 0.8 | 1.1 | 0.862 | 21 |
| Block7 | 74 | 0.26 | 45 | 0.8 | 1 | 0.865 | 20 |
| Block8 | 77 | 0.26 | 45 | 0.8 | 1 | 0.86 | 14 |
| Block9 | 78 | 0.28 | 90 | 0.8 | 1.1 | 0.862 | 21 |
| block10 | 83 | 0.28 | 90 | 0.8 | 1 | 0.862 | 24 |
| Block11+11a | 61 | 0.26 | 45 | 0.69 | 1 | 0.862 | 22 |
| Block12 | 72 | 0.26 | 50 | 0.69 | 1.4 | 0.862 | 12 |
| Block13+15 | 75 | 0.26 | 120 | 0.8 | 1.3 | 0.865 | 22 |
| Block14 | 71 | 0.26 | 80 | 0.74 | 1.1 | 0.865 | 24 |

Table 2. The geological parameters of the blocks

| | Effective Thickness, m | Porosity | Permeability, mD | Oil Saturation | oil viscosity, mPa *s | oil density, g/sm3 | Average pressure of the layer, MPA |
|---------|------------------------|----------|------------------|----------------|-----------------------|--------------------|------------------------------------|
| Block1 | 0.73 | 0 | 0 | 0 | 0.25 | 0.4 | 0.75 |
| Block2 | 0.66 | 0 | 0 | 0 | 0.75 | 1 | 0.75 |
| Block3 | 0 | 0 | 0 | 0 | 0.25 | 0.4 | 0.666 |
| Block4 | 0.3 | 0 | 0 | 0 | 0.5 | 0.4 | 0.666 |
| Block5 | 0.033 | 0 | 0 | 0 | 0 | 0.4 | 0.25 |
| Block6 | 0.733 | 1 | 0.125 | 1 | 0 | 0.4 | 1 |
| Block6a | 0.45 | 0 | 0 | 0 | 0.25 | 0.4 | 0.75 |

| | | | | | | | |
|-------------|-------|-------|-------|---------|------|-----|-------|
| Block7 | 0.85 | 0 | 0.062 | 0.64706 | 0 | 1 | 0.666 |
| Block8 | 0.9 | 0 | 0.062 | 0.64706 | 0 | 0 | 0.166 |
| Block9 | 0.916 | 0.666 | 0.062 | 0.64706 | 0.25 | 0.4 | 0.75 |
| block10 | 1.0 | 0.666 | 0.062 | 0.64706 | 0 | 0.4 | 1 |
| Block11+11a | 0.633 | 0 | 0.062 | 0 | 0 | 0.4 | 0.833 |
| Block12 | 0.816 | 0 | 0.125 | 0 | 1 | 0.4 | 0 |
| Block13+15 | 0.866 | 0 | 1 | 0.64706 | 0.75 | 1 | 0.833 |
| Block14 | 0.8 | 0 | 0.5 | 0.29412 | 0.25 | 1 | 1 |

Table 3. The geological parameters of the blocks after the normalization.

3.3. Results of the clustering

The results of the separate group of the clustering is demonstrated below:

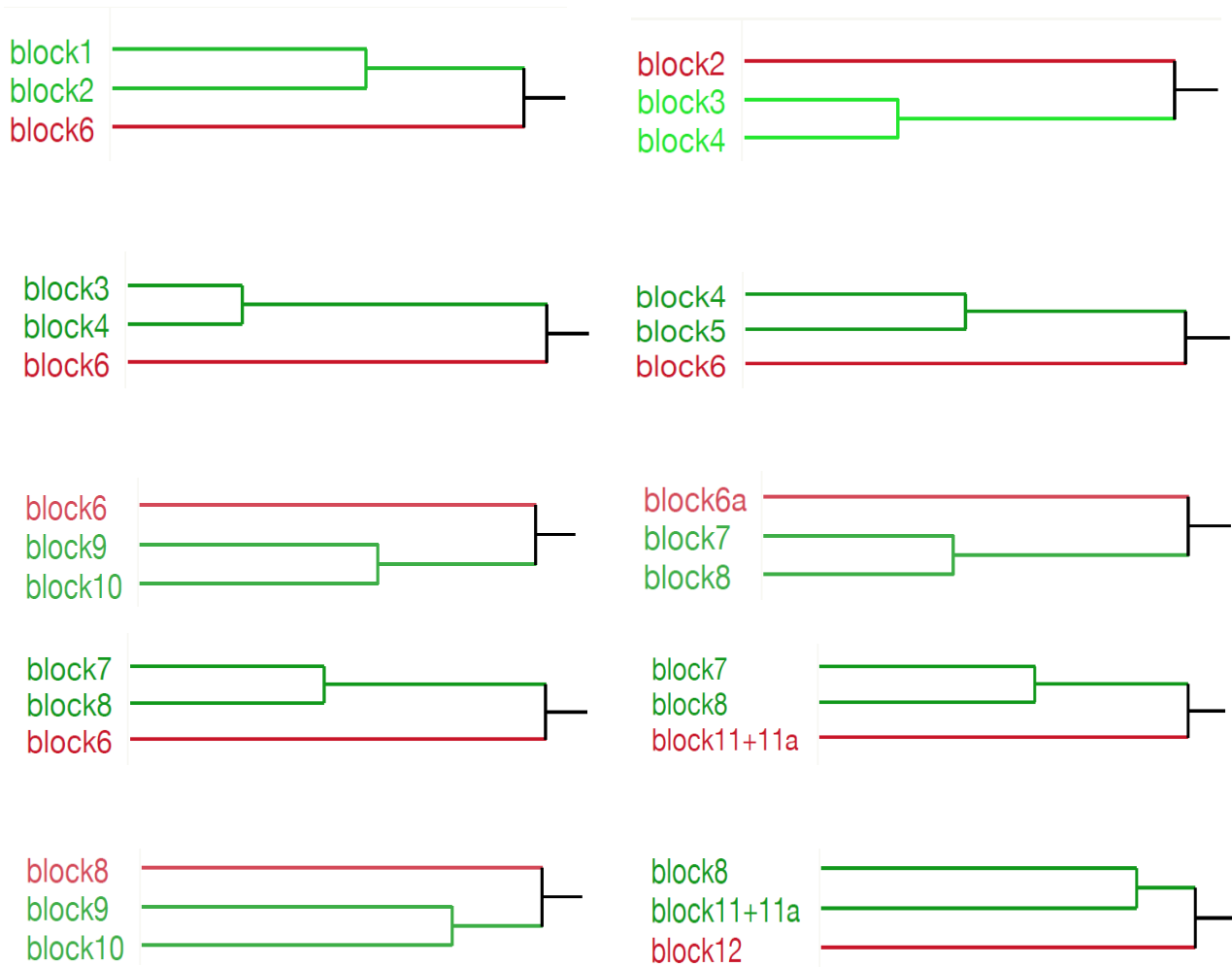


Figure 12. The clusters of the blocks.

Therefore, analysing these dendrograms and at the same time comparing the 2D Model, for instance the blocks 1 and 2 are sharing a transmissible tectonic fault and at the same time block 6 has a non-

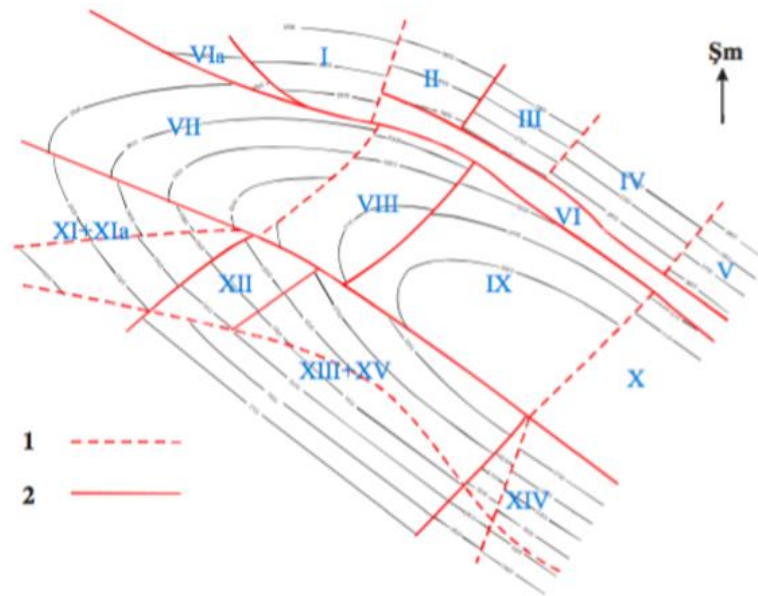


Figure 13. The 2D Model of the shallow depth “Guneshli” field. (OĞLU 2016)p.33(1-transmissible fault, 2- sealing fault).

transmissible tectonic fault with block 2. And obviously the centrally located blocks 8 and 9 blocks are sharing a non-transmissible fault and blocks 9 and 10 transmissible according to the 2D model and Cluster analysis. So, in this case the study of the clusters coincides with the study of the 2D model of the blocks that proves the previous study has been made by SOCAR.

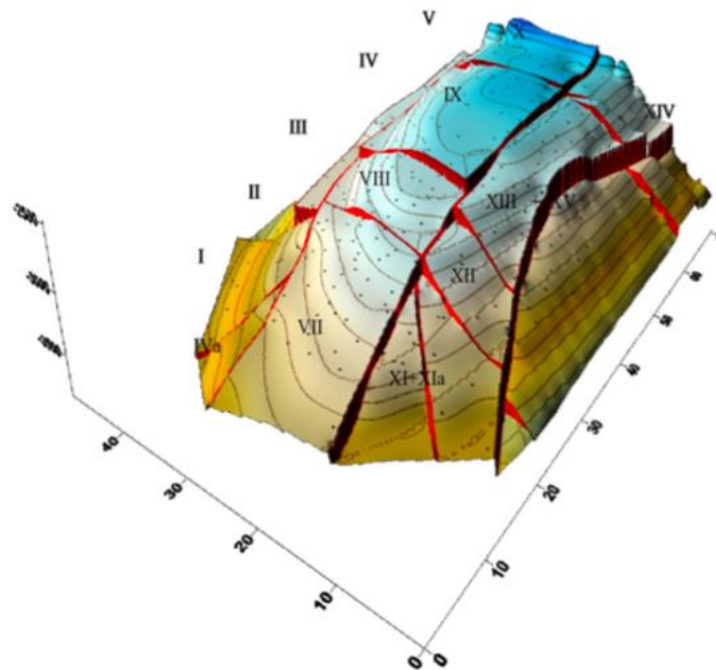


Figure 14. The 3D Model of the shallow depth Guneshli offshore field. (OĞLU 2016)

The 3D Model of the shallow depth “Guneshli” offshore field shows how the blocks are separated between each other due to tectonic faults that are transmissible and sealing.

3.4. Calculation of Oil and Gas Reserves

The initial step was to calculate the volume of hydrocarbons in place (OIP) of the shallow depth “Guneshli” field with the recent data provided from the SOCAR company. Due to the confidentiality agreement with the SOCAR company, the name of the blocks of the shallow depth “Guneshli” offshore field given below are replaced with the A, B, C, D, E, F, G and H letters. The given the data below has been provided by the SOCAR company and it was simulated with the Monte Carlo method for the all given uncertain geological parameters such as Area, Effective thickness, Porosity, Oil Saturation, Formation Volume Factor, Oil Density, GOR as an input data, in order to define the distribution of P90, P50 and P10 in terms of the reserves. Mentioned geological parameters are used as an input data in this software to generate the distribution of the inputs applying rectangular, triangular and normal probability dispersion. The tables below are the volumetric parameters of the hypothetical blocks A, B, C, D, E, F, G and H.

| | Area, 10 ³ m ² | Effective thickness, m | Porosity, % | Oil Saturation, % | Formation Volume Factor | Oil Density, g/sm ³ | GOR, m ³ /ton |
|---------|---|------------------------------|----------------|-------------------------|-------------------------------|--------------------------------------|-----------------------------|
| Minimum | 520 | 24 | 24 | 57 | 1,333 | 0,911 | 200 |
| Mean | 520 | 28 | | | | | |
| Maximum | 3430 | 28 | | | | | |

Table 4. The volumetric data for the layer A.

| | Area, 10 ³ m ² | Effective thickness, m | Porosity, % | Oil Saturation, % | Formation Volume Factor | Oil Density, g/sm ³ | GOR, m ³ /ton |
|---------|---|------------------------------|----------------|-------------------------|-------------------------------|--------------------------------------|-----------------------------|
| Minimum | 1875 | 28 | 25 | 59 | 1,241 | 0,899 | 125 |
| Mean | 1875 | 24 | | | | | |

| | | | | | | | |
|---------|------|----|--|--|--|--|--|
| Maximum | 5375 | 32 | | | | | |
|---------|------|----|--|--|--|--|--|

Table 5. The volumetric data for the layer B.

| | Area, 10 ³ m ² | Effective thickness, m | Porosity, % | Oil Saturation, % | Formation Volume Factor | Oil Density, g/sm ³ | GOR, m ³ /ton |
|---------|---|------------------------------|----------------|-------------------------|-------------------------------|--------------------------------------|-----------------------------|
| Minimum | 13412 | 12 | 24 | 57 | 1,335 | 0,868 | 163 |
| Mean | 13412 | 20 | | | | | |
| Maximum | 21382 | 31 | | | | | |

Table 6. The volumetric data for the layer C.

| | Area, 10 ³ m ² | Effective thickness, m | Porosity, % | Oil Saturation, % | Formation Volume Factor | Oil Density, g/sm ³ | GOR, m ³ /ton |
|---------|---|------------------------------|----------------|-------------------------|-------------------------------|--------------------------------------|-----------------------------|
| Minimum | 23230 | 19 | 26 | 69 | 1,335 | 0,862 | 175 |
| Mean | 23230 | 33 | | | | | |
| Maximum | 25410 | 40 | | | | | |

Table 7. The volumetric data for the layer D.

| | Area, 10 ³ m ² | Effective thickness, m | Porosity, % | Oil Saturation, % | Formation Volume Factor | Oil Density, g/sm ³ | GOR, m ³ /ton |
|---------|---|------------------------------|----------------|-------------------------|-------------------------------|--------------------------------------|-----------------------------|
| Minimum | 24964 | 67 | 26 | 69 | 1,333 | 0,862 | 175 |
| Mean | 24964 | 75 | | 74 | | | |
| Maximum | 25314 | 83 | | 80 | | | |

Table 8. The volumetric data for the layer E.

| | Area, 10 ³ m ² | Effective thickness, m | Porosity, % | Oil Saturation, % | Formation Volume Factor | Oil Density, g/sm ³ | GOR, m ³ /ton |
|---------|---|------------------------------|----------------|-------------------------|-------------------------------|--------------------------------------|-----------------------------|
| Minimum | 510 | 5,5 | | | | | |

| | | | | | | | |
|---------|------|----|----|----|-------|-------|-----|
| Mean | 510 | 9 | 21 | 62 | 1,333 | 0,862 | 257 |
| Maximum | 6980 | 18 | | | | | |

Table 9. The volumetric data for the layer F.

| | Area, 10 ³ m ² | Effective thickness, m | Porosity, % | Oil Saturation, % | Formation Volume Factor | Oil Density, g/sm ³ | GOR, m ³ /ton |
|---------|--------------------------------------|------------------------|-------------|-------------------|-------------------------|--------------------------------|--------------------------|
| Minimum | 6570 | 24 | 24 | 63 | 1,433 | 0,878 | 257 |
| Mean | 6570 | 31 | | | | | |
| Maximum | 8020 | 36 | | | | | |

Table 10. The volumetric data for the layer G.

| | Area, 10 ³ m ² | Effective thickness, m | Porosity, % | Oil Saturation, % | Formation Volume Factor | Oil Density, g/sm ³ | GOR, m ³ /ton |
|---------|--------------------------------------|------------------------|-------------|-------------------|-------------------------|--------------------------------|--------------------------|
| Minimum | 2710 | 22 | 19 | 69 | 1,464 | 0,893 | 248 |
| Mean | 2710 | 36 | | | | | |
| Maximum | 3970 | 47 | | | | | |

Table 11. The volumetric data for the layer H.

The initial step was to calculate the volume of hydrocarbons in place (OIP) of the shallow depth “Guneshli” field with the recent data provided from the SOCAR company. Due to the confidential agreement the mentioned blocks are named as A, B, C, D, E, F, G, H. Following step allows for each block to calculate the Oil and Gas Condensate reserves with the equation below:

$$OOIP = \frac{A \times h \times \phi \times (1 - S_w)}{B_o}$$

| | Block | | | | | | | |
|--|-------|---|---|---|---|---|---|---|
| | A | B | C | D | E | F | G | H |
| | | | | | | | | |

| | | | | | | | | |
|--------------------------------|------|------|-------|-------|--------|-----|-------|------|
| Oil Reserves, M ton | 1361 | 4808 | 23859 | 88800 | 232947 | 386 | 18868 | 7802 |
| Gas reserves,MM m ³ | 272 | 601 | 3889 | 15540 | 40766 | 99 | 4849 | 1935 |

Table 12. Calculated the Oil and Gas Reserves for each layer.

At the end the total Oil and Gas Reserves has been calculated for the all blocks the results is demonstrated in the below tables:

| | M ton | MM bbl |
|--------------|--------|--------|
| Oil Reserves | 378831 | 2591 |

Table 13. The total oil reserves.

| | MM m ³ | Bcf |
|--------------|-------------------|------|
| Gas Reserves | 67951 | 2399 |

Table 14. The total gas reserves.

3.5. Monte Carlo Simulation of the Calculated OIP with Crystal Ball Software

In order to make these analyses to the deterministic level, the use of software called Crystal Ball has been applied. Mentioned geological parameters are used as an input data in this software to generate the distribution of the inputs applying rectangular, triangular and normal probability dispersion. Running this software allows to build various scenarios starting from Optimistic reserve values (P90), promising reserve values (P50) to Pessimistic reserve values (P10). The simulation Monte Carlo simulation results has been extracted as a report, the number of trials has been set to 10000.

Here, Crystal Ball allows not only the reserve estimation but also to run a sensitivity analysis of the input parameters, how each parameter impacts the estimation of the recoverable reserves.

Summary:

Entire range is from 308,113.51 to
495,996.56

Base case is 378,831.45

After 10,000 trials, the std. error of the mean is 266.96

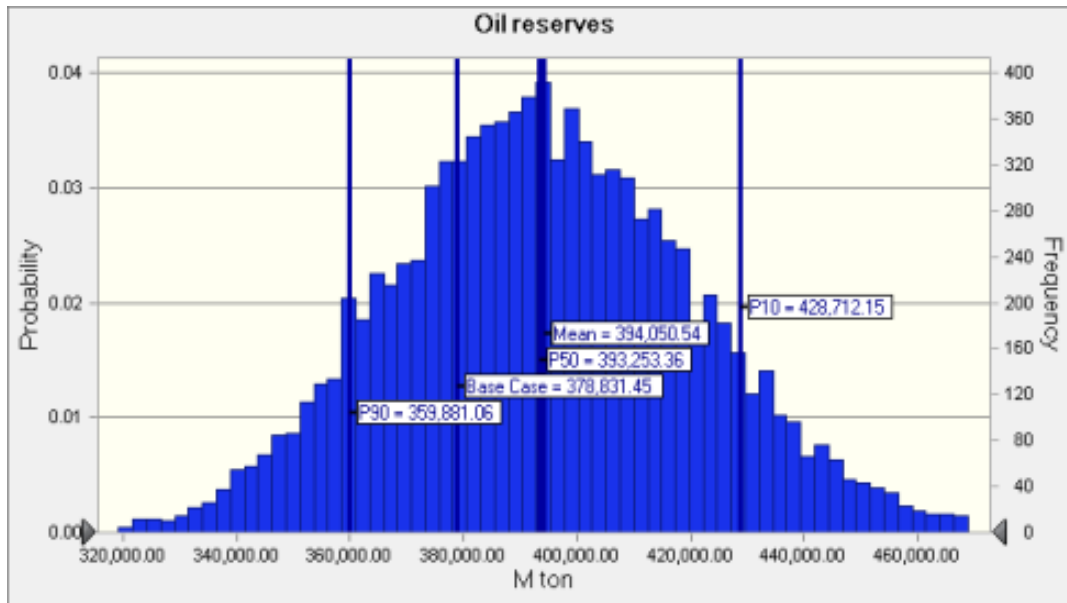


Figure 15. Monte Carlo distribution of oil reserves (M ton) in terms of P90, P50, P10.

| Statistics | Forecast values, M ton |
|---------------------|------------------------|
| Trials | 378,831.45 |
| Base Case | 394,050.54 |
| Mean | 393,255.57 |
| Median | --- |
| Mode | 26,696.23 |
| Standard Deviation | 712,688,497.95 |
| Variance | 0.1244 |
| Skewness | 2.94 |
| Kurtosis | 0.0677 |
| Coeff. of Variation | 308,113.51 |
| Minimum | 495,996.56 |
| Maximum | 187,883.05 |
| Range Width | 266.96 |
| Mean Std. Error | 378,831.45 |
| Base Case | 394,050.54 |

Table 15. The Forecast values of the Monte Carlo simulation.

| Percentiles | Forecast values, M ton |
|-------------|------------------------|
| P100 | 308,113.51 |
| P90 | 359,881.06 |
| P80 | 371,434.45 |
| P70 | 379,679.34 |
| P60 | 386,712.56 |
| P50 | 393,253.36 |

| | |
|-----|------------|
| P40 | 400,130.23 |
| P30 | 407,733.96 |
| P20 | 416,457.44 |
| P10 | 428,712.15 |
| P0 | 495,996.56 |

Table 16. The vary of results of the Monte Carlo simulation of oil reserves(M ton) forecast (in percentiles).

In terms of MM bbl the outcome of the Monte Carlo Simulation:

Entire range is from 2107 to 3393 and the Base case is 2591.

After 10,000 trials, the std. error of the mean is 2.

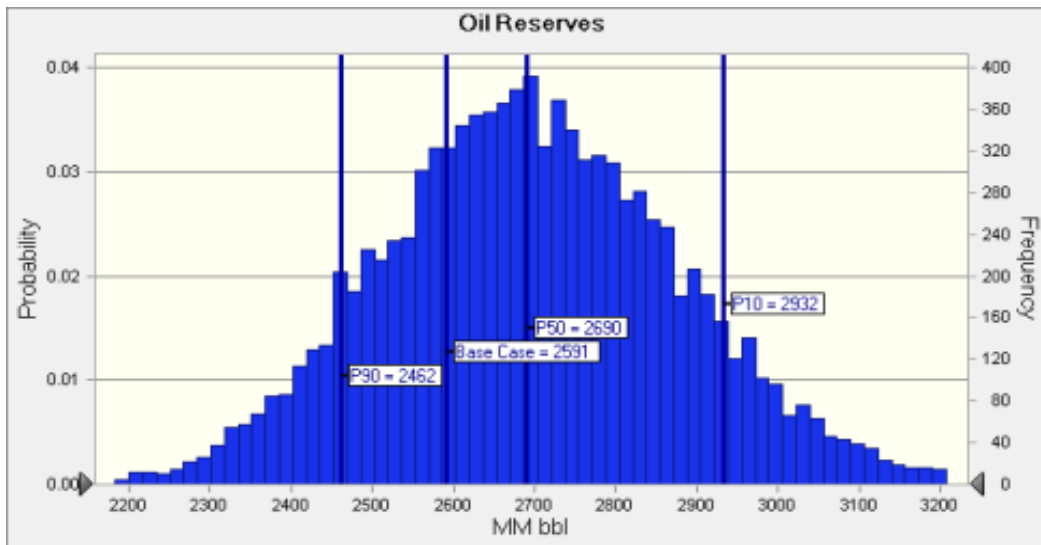


Figure 16. Monte Carlo distribution of oil reserves (MM bbl) in terms of P90, P50, P10.

| Statistics | Forecast values, M ton |
|---------------------|------------------------|
| Trials | 10,000 |
| Base Case | 2591 |
| Mean | 2695 |
| Median | 2690 |
| Mode | --- |
| Standard Deviation | 183 |
| Variance | 33344 |
| Skewness | 0.1244 |
| Kurtosis | 2.94 |
| Coeff. of Variation | 0.0677 |
| Minimum | 2107 |
| Maximum | 3393 |
| Range Width | 1285 |
| Mean Std. Error | 2 |

Table 17. The Forecast values of the Monte Carlo simulation.

| Percentiles | Forecast values, MM bbl |
|-------------|-------------------------|
| P100 | 2107 |
| P90 | 2462 |
| P80 | 2541 |
| P70 | 2597 |
| P60 | 2645 |
| P50 | 2690 |
| P40 | 2737 |
| P30 | 2789 |
| P20 | 2849 |
| P10 | 2932 |
| P0 | 3393 |

Table 18. The vary of results of the Monte Carlo simulation of oil reserves(MM bbl) forecast (in percentiles).

For the Gas Reserves:

Entire range is from 53,717.97 to 91,473.03 and the Base case is 67,951.20.

After 10,000 trials, the std. error of the mean is 50.23.

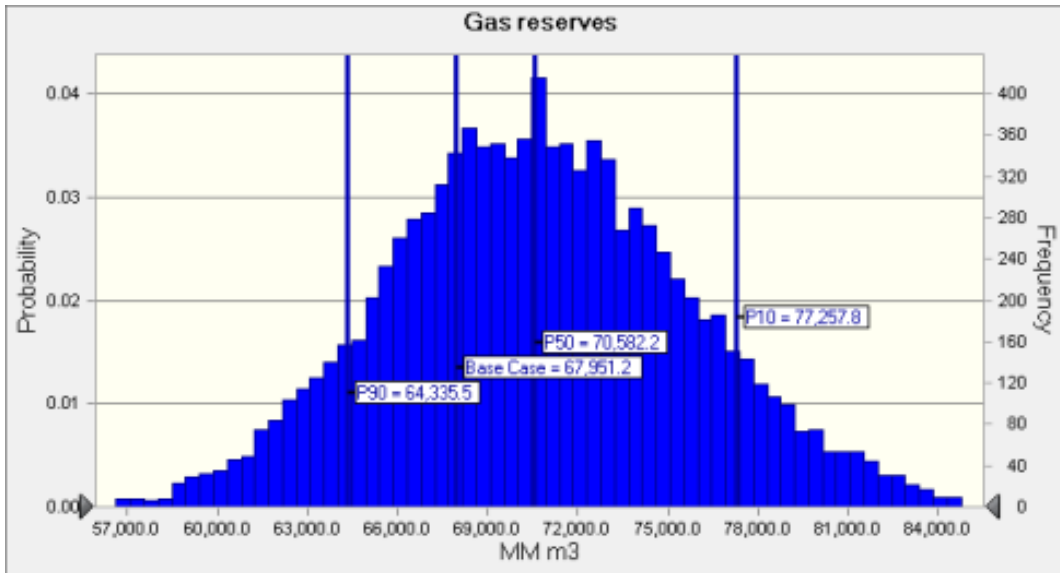


Figure 17. Monte Carlo distribution of gas reserves (MM m³) in terms of P90, P50, P10.

| Statistics | Forecast values, m ³ |
|---------------------|---------------------------------|
| Trials | 10,000 |
| Base Case | 67,951.20 |
| Mean | 70,698.28 |
| Median | 70,582.20 |
| Mode | --- |
| Standard Deviation | 5,022.94 |
| Variance | 25,229,916.78 |
| Skewness | 0.1270 |
| Kurtosis | 2.96 |
| Coeff. of Variation | 0.0710 |
| Minimum | 53,717.97 |
| Maximum | 91,473.03 |
| Range Width | 37,755.06 |
| Mean Std. Error | 50.23 |

Table 19. The Forecast values of the Monte Carlo simulation

| Percentiles | Forecast values, m ³ |
|-------------|---------------------------------|
| P100 | 53,717.97 |
| P90 | 64,335.49 |
| P80 | 66,479.19 |
| P70 | 68,008.40 |
| P60 | 69,291.93 |
| P50 | 70,582.16 |
| P40 | 71,831.70 |
| P30 | 73,207.75 |
| P20 | 74,900.65 |
| P10 | 77,257.84 |
| P0 | 91,473.03 |

Table 20. The vary of results of the Monte Carlo simulation of gas reserves (m3) forecast (in percentiles).

In terms Bcf:

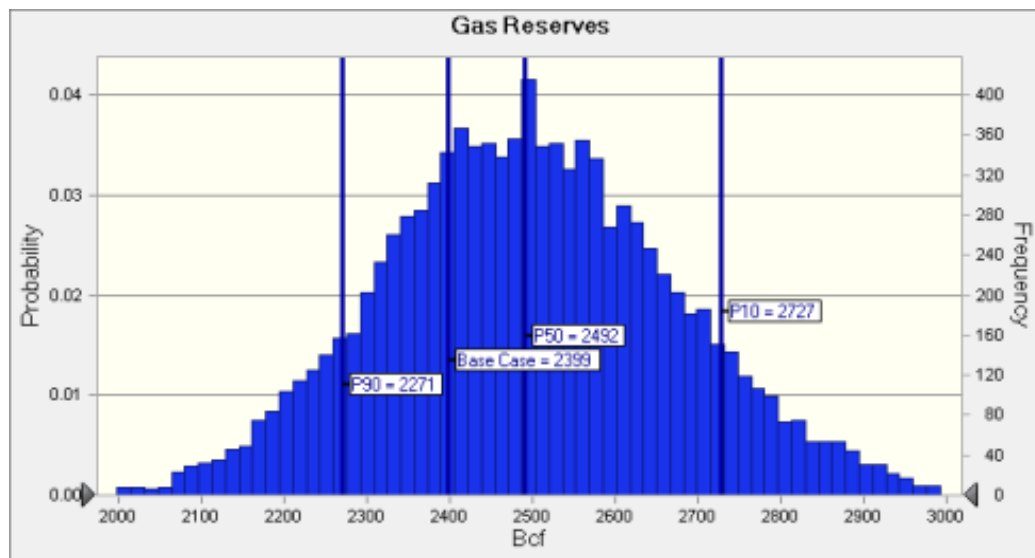


Figure 18. Monte Carlo distribution of gas reserves (Bcf) in terms of P90, P50, P10

Entire range is from 1896 to 3229

Base case is 2399

After 10,000 trials, the std. error of the mean is 2

One of the aims of this this simulation was to compare the Oil and Gas Reserves Estimation using Crystal Ball software with the Mball software that was applied by the Senior Geologist in SOCAR to simulate Monte Carlo method in order to obtain the Reserves estimation.

| Percentiles | Forecast values, Bcf |
|-------------|----------------------|
| P100 | 1896 |
| P90 | 2271 |
| P80 | 2347 |
| P70 | 2401 |
| P60 | 2446 |
| P50 | 2492 |
| P40 | 2536 |
| P30 | 2584 |
| P20 | 2644 |
| P10 | 2727 |
| P0 | 3229 |

Table 21. The vary of results of the Monte Carlo simulation of gas reserves (Bcf) forecast (in percentiles).

Below the table shows the comparison of the results of the Crystal Ball and the Mball, respectively.

| | P10 | P50 | P90 | Methods |
|---------------------------------|--------|--------|--------|--------------|
| Oil Reserves, M Ton | 429036 | 393206 | 360977 | Crystal Ball |
| | 406512 | 355539 | 304449 | M Ball |
| MM bbl | 2935 | 2690 | 2469 | Crystal Ball |
| | 2781 | 2432 | 2082 | M Ball |
| GAS Reserves, MM m ³ | 77289 | 70499 | 64489 | Crystal Ball |
| | 103057 | 90121 | 77206 | M Ball |
| Bscf | 2728 | 2489 | 2276 | Crystal Ball |
| | 3638 | 3181 | 2725 | M Ball |

Table 22. The comparison of the Monte Carlo simulation between softwares Crystal Ball and Mball.

The results provided by Elvin Ahmadov (Senior Geologist in SOCAR) from the Mball Monte Carlo simulation for the Oil reserves and Gas reserves are P10 = 2781 MM bbl, P50 = 2432 MM bbl and P90 = 2082 MM bbl, and P10 = 3638 Bscf, P50 = 3181 Bscf and P90 = 2082 Bscf, respectively.

Conversely the Crystal Ball Monte Carlo simulation concludes that the results are quite different from the Mball Monte Carlo analysis. So the observation from Crystal Ball Monte Carlo simulation can be made that the P10 = 2935 MM bbl, P50 = 2690 MM bbl and P90 = 2469 MM bbl, and P10 = 2728 Bscf, P50 = 2489 Bscf and P90 = 2276 Bscf, respectively.

The comparison demonstrates that in case of Oil reserves the estimation with Crystal Ball overestimates slightly respect to the Mball by approximately 200-400 MM bbl. In case of Gas reserves the Crystal Ball estimation underestimates approximately by 500-1000 Bscf.

3.6. Tornado charts

Tornado charts and Sensitivity charts combine with the Oracle Crystal Ball Monte Carlo runs allows to clearly see the affect of each geological parameter on the defined reserve volumes. In this case each bar of the Tornado Chart demonstrates the upside and the downside volumetric impact of a specific geological parameter such as Effective thickness, Oil Saturation, Area, Porosity, oil density and the Formation Volume Factor of each layer.

For instance, each bar of the provided Tornado Chart correlates to an independent uncertain parameter. Here, the assumption can be made that The Effective thickness of the layer D has the highest sensitivity ranking and is the most important which means higher uncertainty. The effective thickness of the layer E below should also be considered as it is in the high sensitivity ranking. Further, the parameter such as Oil saturation of the layer E as a different parameter from the previous ones has also a significant impact.

The last parameters after the parameter Area of the layer E, have the least influence on the sensitivity ranking and can be ignored in further analysis.

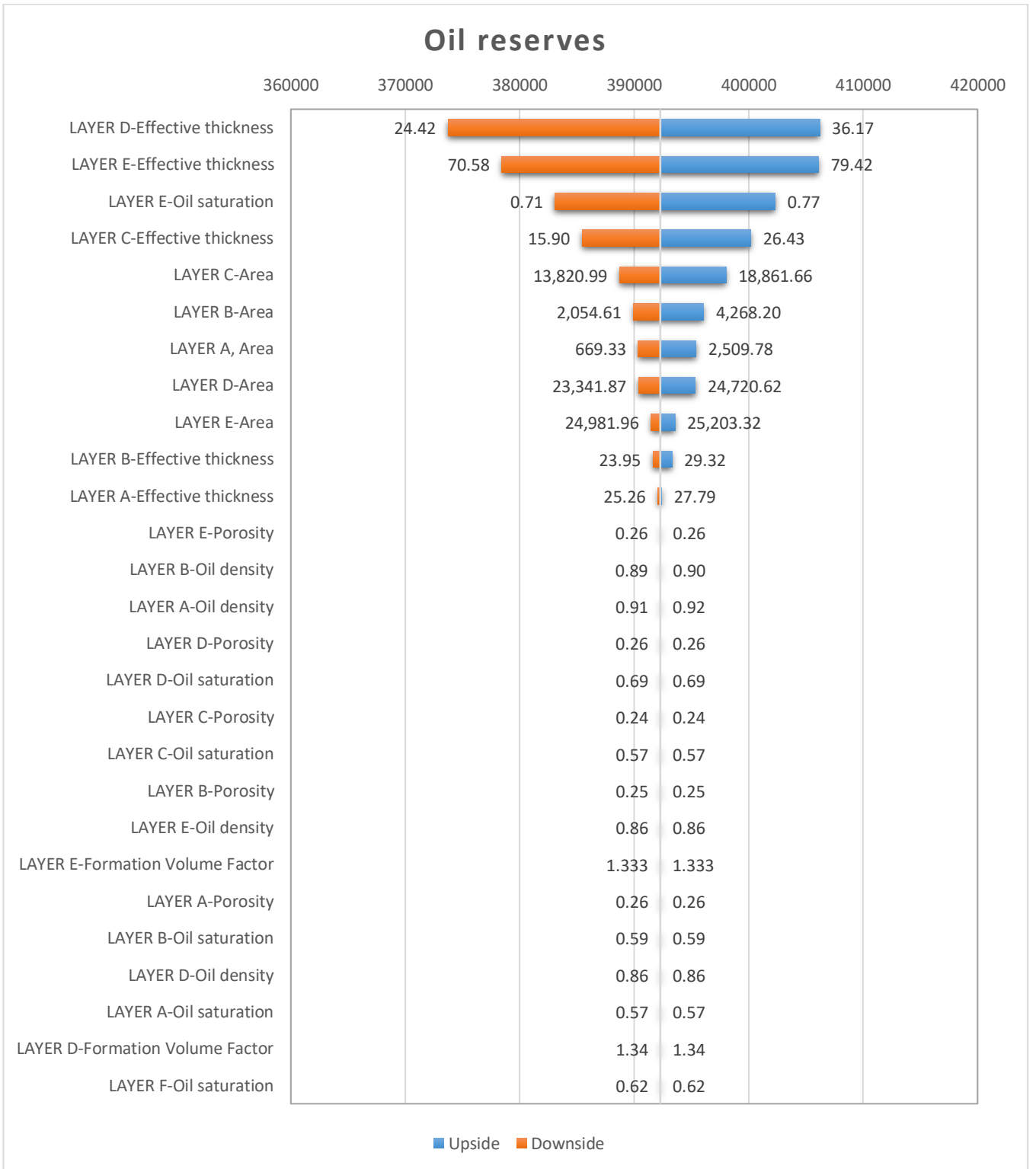


Figure 19. Tornado chart of Oil Reserves.

| Input Variable | reserves | | | | Explained Variation ¹ | Input | | |
|---------------------------------|----------|--------|-------|----------|-------------------------------------|-----------|-----------|--|
| | Downside | Upside | Range | Downside | | Upside | Base Case | |
| LAYER D-Effective thickness | 373744 | 406222 | 32479 | 39.84% | 24.42 | 36.17 | 31.12 | |
| LAYER E-Effective thickness | 378437 | 406121 | 27684 | 68.79% | 70.58 | 79.42 | 75.00 | |
| LAYER E-Oil saturation | 383078 | 402318 | 19240 | 82.77% | 0.71 | 0.77 | 0.74 | |
| LAYER C-Effective thickness | 385444 | 400196 | 14752 | 90.99% | 15.90 | 26.43 | 20.78 | |
| LAYER C-Area | 388720 | 398038 | 9318 | 94.27% | 13,820.99 | 18,861.66 | 15,746.36 | |
| LAYER B-Area | 389940 | 396064 | 6124 | 95.68% | 2,054.61 | 4,268.20 | 2,900.13 | |
| LAYER A, Area | 390359 | 395386 | 5027 | 96.64% | 669.33 | 2,509.78 | 1,372.32 | |
| LAYER D-Area | 390380 | 395352 | 4972 | 97.57% | 23,341.87 | 24,720.62 | 23,868.51 | |
| LAYER G-Effective thickness | 389957 | 394269 | 4312 | 98.27% | 26.90 | 33.55 | 30.48 | |
| LAYER F-Area | 390895 | 394519 | 3624 | 98.77% | 842.02 | 4,934.01 | 2,405.02 | |
| LAYER H-Effective thickness | 390478 | 393887 | 3409 | 99.21% | 27.92 | 41.76 | 35.23 | |
| LAYER G-Area | 391290 | 393880 | 2590 | 99.46% | 6,644.41 | 7,561.47 | 6,994.70 | |
| LAYER H-Area | 391421 | 393667 | 2246 | 99.65% | 2,774.66 | 3,571.55 | 3,079.05 | |
| LAYER E-Area | 391487 | 393560 | 2073 | 99.81% | 24,981.96 | 25,203.32 | 25,066.51 | |
| LAYER B-Effective thickness | 391646 | 393303 | 1657 | 99.92% | 23.95 | 29.32 | 26.00 | |
| LAYER F-Effective thickness | 391693 | 393117 | 1424 | 99.99% | 7.62 | 14.65 | 10.52 | |
| LAYER A-Effective thickness | 392061 | 392414 | 353 | 100.00% | 25.26 | 27.79 | 26.83 | |
| LAYER E-Porosity | 392243 | 392315 | 72 | 100.00% | 0.26 | 0.26 | 0.26 | |
| LAYER B-Oil density | 392243 | 392315 | 72 | 100.00% | 0.89 | 0.90 | 0.90 | |
| LAYER A-Oil density | 392264 | 392294 | 29 | 100.00% | 0.91 | 0.92 | 0.92 | |
| LAYER D-Porosity | 392266 | 392292 | 26 | 100.00% | 0.26 | 0.26 | 0.26 | |
| LAYER D-Oil saturation | 392274 | 392284 | 10 | 100.00% | 0.69 | 0.69 | 0.69 | |
| LAYER C-Porosity | 392274 | 392284 | 10 | 100.00% | 0.24 | 0.24 | 0.24 | |
| LAYER G-Porosity | 392276 | 392282 | 7 | 100.00% | 0.24 | 0.24 | 0.24 | |
| LAYER C-Oil saturation | 392277 | 392281 | 4 | 100.00% | 0.57 | 0.57 | 0.57 | |
| LAYER H-Porosity | 392277 | 392281 | 4 | 100.00% | 0.19 | 0.19 | 0.19 | |
| LAYER B-Porosity | 392278 | 392280 | 3 | 100.00% | 0.25 | 0.25 | 0.25 | |
| LAYER G-Oil saturation | 392278 | 392280 | 3 | 100.00% | 0.63 | 0.63 | 0.63 | |
| LAYER E-Oil density | 392278 | 392280 | 2 | 100.00% | 0.86 | 0.86 | 0.86 | |
| LAYER E-Formation Volume Factor | 392280 | 392278 | 1 | 100.00% | 1.333 | 1.333 | 1.333 | |
| LAYER A-Porosity | 392279 | 392280 | 1 | 100.00% | 0.26 | 0.26 | 0.26 | |
| LAYER B-Oil saturation | 392279 | 392280 | 1 | 100.00% | 0.59 | 0.59 | 0.59 | |
| LAYER H-Oil saturation | 392279 | 392280 | 1 | 100.00% | 0.69 | 0.69 | 0.69 | |
| LAYER F-Porosity | 392279 | 392279 | 1 | 100.00% | 0.21 | 0.21 | 0.21 | |
| LAYER D-Oil density | 392279 | 392279 | 1 | 100.00% | 0.86 | 0.86 | 0.86 | |
| LAYER A-Oil saturation | 392279 | 392279 | 1 | 100.00% | 0.57 | 0.57 | 0.57 | |
| LAYER D-Formation Volume Factor | 392279 | 392279 | 1 | 100.00% | 1.34 | 1.34 | 1.34 | |
| LAYER F-Oil saturation | 392279 | 392279 | 0 | 100.00% | 0.62 | 0.62 | 0.62 | |
| LAYER C-Oil density | 392279 | 392279 | 0 | 100.00% | 0.87 | 0.87 | 0.87 | |
| LAYER G-Oil density | 392279 | 392279 | 0 | 100.00% | 0.88 | 0.88 | 0.88 | |

¹ Explained Variation is cumulative

Run options:

| | |
|--------------------------------------|------------------------------|
| Tornado method | Percentiles of the variables |
| Test range | P90 to P10 |
| Test points | 30 |
| Customize test ranges by variable | Off |
| Show top variables | 40 |
| Base case for Crystal Ball variables | Median values |

Table 23. Uncertain variables present in the Tornado chart.

The table above shows the results data of the Tornado Chart where:

- The input variable names in chart order, starting with the variable with the greatest impact on the target
- The downside difference from the base case
- The upside difference from the base case
- The percent of explained variation in the target, approximately equal to statistical variance (R^2), cumulative from the variable with the greatest impact to the least
- The Absolute downside value
- The Absolute upside value
- The base case value

The same analysis has been made to define the impact of the uncertain parameters on the Gas Reserves.

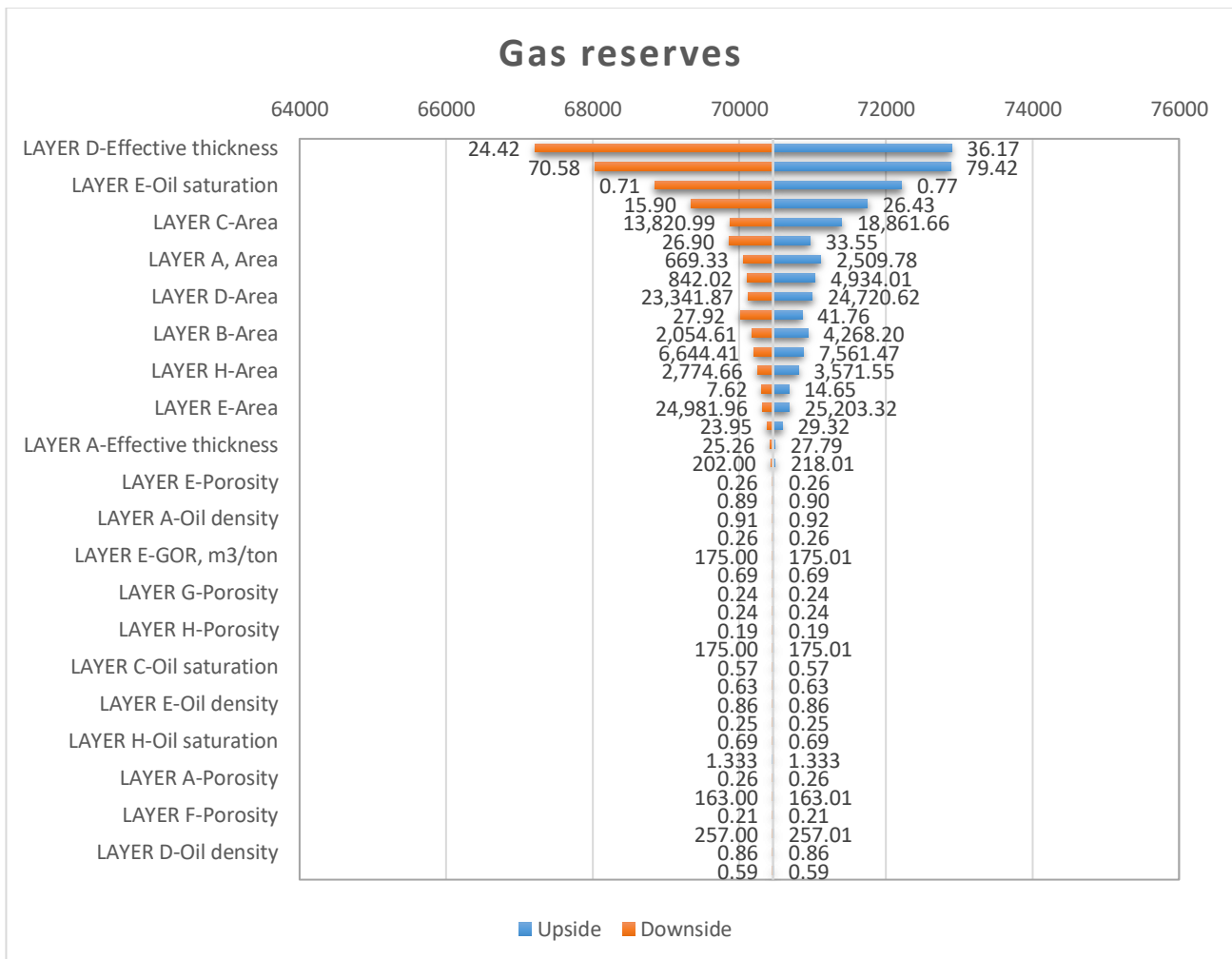


Figure 20. Tornado chart of Gas reserves.

From the demonstrated Tornado Chart the slight difference can be observed and clearly the Effective Thickness of the layers D and E are the most significant uncertain parameters to define the Gas Reserves volumes. The affect of the Area of the layers C, A, D, B, H and D are comparably small. And the effect of the other below parameters can be neglected as they are very minor.

| Input Variable | Gas reserves | | | | Input | | |
|---------------------------------|--------------|--------|-------|----------------------------------|-----------|-----------|-----------|
| | Downside | Upside | Range | Explained Variation ¹ | Downside | Upside | Base Case |
| LAYER D-Effective thickness | 67216 | 72900 | 5684 | 39.62% | 24.42 | 36.17 | 31.12 |
| LAYER E-Effective thickness | 68037 | 72882 | 4845 | 68.40% | 70.58 | 79.42 | 75.00 |
| LAYER E-Oil saturation | 68850 | 72217 | 3367 | 82.31% | 0.71 | 0.77 | 0.74 |
| LAYER C-Effective thickness | 69346 | 71750 | 2405 | 89.40% | 15.90 | 26.43 | 20.78 |
| LAYER C-Area | 69879 | 71398 | 1519 | 92.23% | 13,820.99 | 18,861.66 | 15,746.36 |
| LAYER G-Effective thickness | 69863 | 70971 | 1108 | 93.73% | 26.90 | 33.55 | 30.48 |
| LAYER A, Area | 70056 | 71112 | 1056 | 95.10% | 669.33 | 2,509.78 | 1,372.32 |
| LAYER F-Area | 70104 | 71035 | 931 | 96.16% | 842.02 | 4,934.01 | 2,405.02 |
| LAYER D-Area | 70127 | 70997 | 870 | 97.09% | 23,341.87 | 24,720.62 | 23,868.51 |
| LAYER H-Effective thickness | 70013 | 70858 | 845 | 97.97% | 27.92 | 41.76 | 35.23 |
| LAYER B-Area | 70167 | 70933 | 766 | 98.69% | 2,054.61 | 4,268.20 | 2,900.13 |
| LAYER G-Area | 70205 | 70871 | 666 | 99.23% | 6,644.41 | 7,561.47 | 6,994.70 |
| LAYER H-Area | 70247 | 70804 | 557 | 99.61% | 2,774.66 | 3,571.55 | 3,079.05 |
| LAYER F-Effective thickness | 70309 | 70675 | 366 | 99.77% | 7.62 | 14.65 | 10.52 |
| LAYER E-Area | 70321 | 70684 | 363 | 99.94% | 24,981.96 | 25,203.32 | 25,066.51 |
| LAYER B-Effective thickness | 70381 | 70588 | 207 | 99.99% | 23.95 | 29.32 | 26.00 |
| LAYER A-Effective thickness | 70414 | 70488 | 74 | 100.00% | 25.26 | 27.79 | 26.83 |
| LAYER A-GOR, m3/ton | 70430 | 70490 | 60 | 100.00% | 202.00 | 218.01 | 210.01 |
| LAYER E-Porosity | 70453 | 70466 | 13 | 100.00% | 0.26 | 0.26 | 0.26 |
| LAYER B-Oil density | 70455 | 70464 | 9 | 100.00% | 0.89 | 0.90 | 0.90 |
| LAYER A-Oil density | 70457 | 70463 | 6 | 100.00% | 0.91 | 0.92 | 0.92 |
| LAYER D-Porosity | 70457 | 70462 | 5 | 100.00% | 0.26 | 0.26 | 0.26 |
| LAYER E-GOR, m3/ton | 70459 | 70461 | 2 | 100.00% | 175.00 | 175.01 | 175.01 |
| LAYER D-Oil saturation | 70459 | 70461 | 2 | 100.00% | 0.69 | 0.69 | 0.69 |
| LAYER G-Porosity | 70459 | 70461 | 2 | 100.00% | 0.24 | 0.24 | 0.24 |
| LAYER C-Porosity | 70459 | 70460 | 2 | 100.00% | 0.24 | 0.24 | 0.24 |
| LAYER H-Porosity | 70459 | 70460 | 1 | 100.00% | 0.19 | 0.19 | 0.19 |
| LAYER D-GOR, m3/ton | 70459 | 70460 | 1 | 100.00% | 175.00 | 175.01 | 175.01 |
| LAYER C-Oil saturation | 70459 | 70460 | 1 | 100.00% | 0.57 | 0.57 | 0.57 |
| LAYER G-Oil saturation | 70459 | 70460 | 1 | 100.00% | 0.63 | 0.63 | 0.63 |
| LAYER E-Oil density | 70459 | 70460 | 0 | 100.00% | 0.86 | 0.86 | 0.86 |
| LAYER B-Porosity | 70460 | 70460 | 0 | 100.00% | 0.25 | 0.25 | 0.25 |
| LAYER H-Oil saturation | 70460 | 70460 | 0 | 100.00% | 0.69 | 0.69 | 0.69 |
| LAYER E-Formation Volume Factor | 70460 | 70460 | 0 | 100.00% | 1.333 | 1.333 | 1.333 |
| LAYER A-Porosity | 70460 | 70460 | 0 | 100.00% | 0.26 | 0.26 | 0.26 |
| LAYER C-GOR, m3/ton | 70460 | 70460 | 0 | 100.00% | 163.00 | 163.01 | 163.01 |
| LAYER F-Porosity | 70460 | 70460 | 0 | 100.00% | 0.21 | 0.21 | 0.21 |
| LAYER G-GOR, m3/ton | 70460 | 70460 | 0 | 100.00% | 257.00 | 257.01 | 257.01 |
| LAYER D-Oil density | 70460 | 70460 | 0 | 100.00% | 0.86 | 0.86 | 0.86 |
| LAYER B-Oil saturation | 70460 | 70460 | 0 | 100.00% | 0.59 | 0.59 | 0.59 |

¹ Explained Variation is cumulative

Run options:

| | |
|--------------------------------------|------------------------------|
| Tornado method | Percentiles of the variables |
| Test range | P90 to P10 |
| Test points | 30 |
| Customize test ranges by variable | Off |
| Show top variables | 40 |
| Base case for Crystal Ball variables | Median values |

Table 24. Uncertain variables present in the Tornado chart.

Another important aspect is followed by the definition of the Sensitivity Chart. The “Sensitivity Chart” builds a ranking of the assumptions from the most important to the least important in the model, based on the consequence.

The presented Sensitivity Chart coincides with the Tornado Chart demonstrated previously and the assumption would be a value “20%” of the Effective Thickness of the Layer D which is resulted with the highest sensitivity affect compared with the other parameters. And this will have a significant impact on the forecasting.

Moving on outcome of the Sensitivity Chart of the Gas Reserves the assumptions are identically same. The only change is the percentage of the values which for the Effective Thickness of the Layer D is 17.2% which is slightly lower than in the case of the Oil Reserves’ the Effective Thickness’ value.

However, in the both cases the Effective thickness of the layer D shows the highest sensitivity impact on the Forecasting.

Despite of the geological parameter Oil Saturation of the layer E is not resulted with the high sensitivity value in the Sensitivity Chart as the Effective Thickness, although the uncertainty bar in the Tornado Chart is in one of the highest levels in both cases, oil and gas reserves.

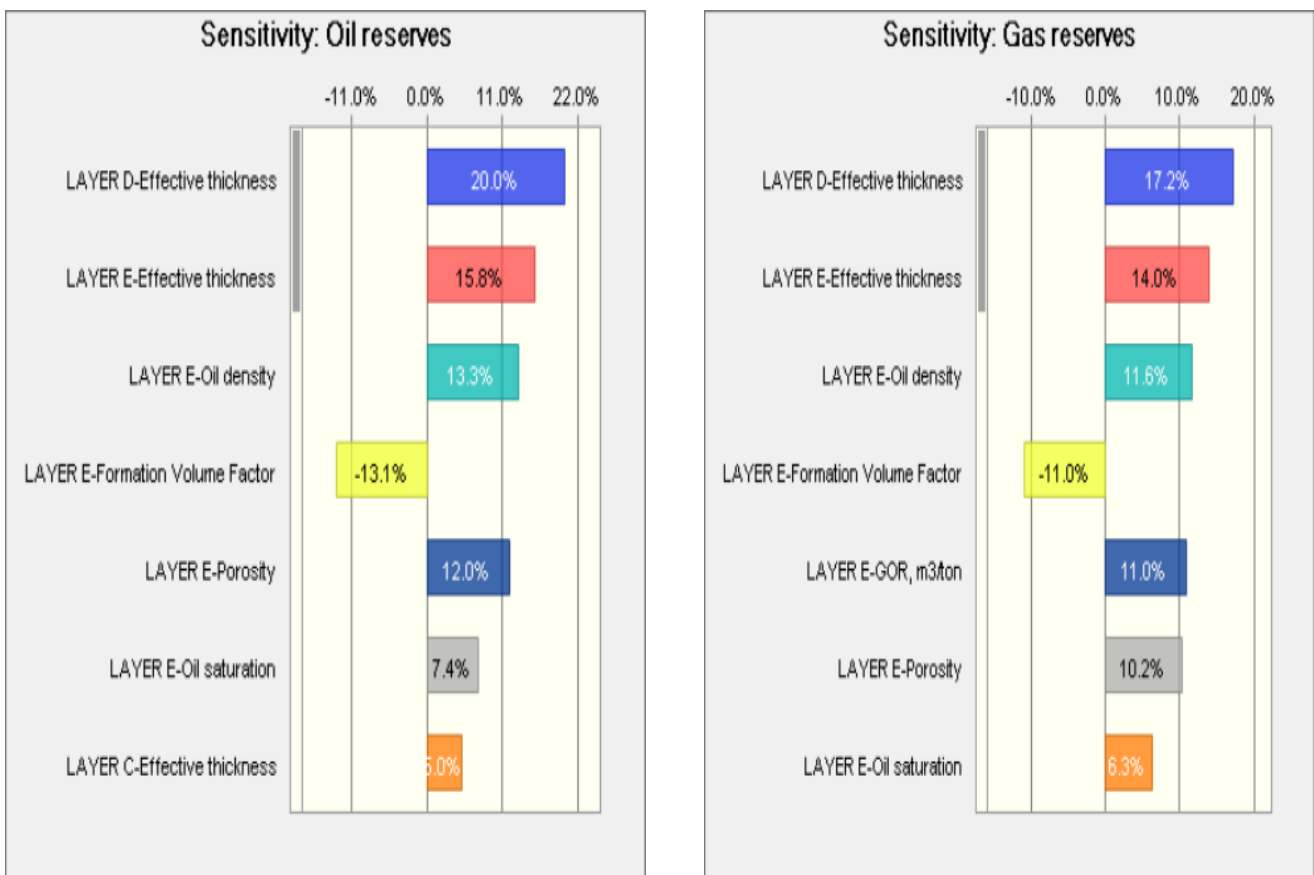


Figure 21. Sensitivity charts of Oil and Gas reserves.

Chapter 4

Conclusions

The purpose of the thesis was to investigate the affect of the geological parameters on the oil and gas reserves estimation with the help of the deterministic method (Monte Carlo Simulation) applying Oracle Crystal Ball software.

The obtained results show that in the case of oil reserves, the following probabilities - P10, P50 and P90 are 2935 MM bbl, 2690 MM bbl and 2469 MM bbl, respectively. In the case of the gas reserves, the following P10, P50 and P90 are 2728 Bscf, 2489 Bscf and 2276 Bscf, respectively. Further, the affect of the parameters was displayed in terms of the Tornado and the Sensitivity charts. After the study and analysis related to the reserves' estimation made in the previous chapters, the conclusions of this research are followings:

1. The Oracle Crystal Ball software is applicable as it can run thousands of trials, in this case with 10,000 trials the Monte Carlo Simulation has been made and the established outcome of the oil and gas reserves estimation in the cases from P10 to P90, the probability in terms of 10% and 90%.
2. Based on the Tornado chart, basically the attention should be made on the Effective thickness and Oil saturation for the layers C, D and E layers of the shallow depth "Guneshli" offshore field when estimating the oil reserves. For the gas reserves estimation, mainly the Effective thickness should be taken into more account.
3. Sensitivity analysis (figure 21) demonstrates the decreasing affect of the parameters from the Effective thickness to the Oil Saturation and the chart presented in percentiles also highlights not only the importance of the Effective thickness parameter in the layers E and D but also the oil density. So, these uncertainties should also be under attention for the further reserves' estimation in the future.
4. The comparison of the software the Oracle Crystal Ball and Mball was one of the scopes of the thesis. The study reviled that the use of the Oracle Crystal Ball is more precise in terms of the forecast and sensitivity analysis of the geological parameters (not only) and the application provided by Oracle has been severely used and tested in the oil field with the various purposes resulting with positive feedbacks.
5. Based on the Hierarchical analysis performed on the geological parameters with the help of JMP software, the transmissibility of the tectonic faults between the blocks has been verified and demonstrated as tree (Figure 14). The used method is not very common, but data analysis

used as an additional method is helpful in the case of already existing 2D or 3D Models where the nature of the tectonic faults has been demonstrated.

Overall, the Oracle Crystal Ball software identifies the geological parameters in this case that minimises uncertainties that affect the hydrocarbon estimation and JMP software resulted with the confirmation of the tectonic faults nature(transmissibility) between the given blocks. Both these softwares are commonly used worldwide by data analysts (not only) in various fields of research and work.

References

1. *JMP Statistical Discovery* . n.d. <https://www.jmp.com/support/help/14-2/distance-method-formulas.shtml#177809>.
2. A.A. Narimanov, Ibrahim Palaz. "OIL HISTORY, POTENTIAL CONVERGE IN AZERBAIJAN." *OIL&GAS JOURNAL*, n.d.
3. A.Narimanov, Michael A.Abrams Akif. "Geochemical evaluation of hydrocarbons and their potential sources in the western South Caspian depression." n.d.
4. Arvin Khadem Samimi, Ghafoor Karimi. *SENSITIVITY & UNCERTAINTY ANALYSIS OF ORIGINAL OIL-IN-PLACE IN CARBONATE RESERVOIR MODELING, A CASE STUDY*. Petroleum & Coal ISSN 1337-7027, 2014.
5. *AureaWorks- Quantitative Risk Analysis and Modeling Techniques*. December 4, 2016. <https://community.jivesoftware.com/docs/DOC-216664>.
6. Auwalu Inuwa Mohammed, Hassan Abdurahman, Sulaiman Dodo Ibrahim, Bello Mohammed Adamu. "Uncertainty Modelling in Multi-Layered Reserve Estimation Using Monte Carlo Simulation ." *SPE - 193454 - MS* , 2018: p. 12.
7. B. Corre, P. Thore, V. de Feraudy and G. Vincent, SPE, TOTALFINA ELF. "Integrated Uncertainty Assessment For Project Evaluation and Risk Analysis." *SPE 65205*, 2000: p. 9.
8. B.Ə., Bağırov. "AZƏRBAYCAN NEFT YATAQLARININ İŞLƏNİLMƏSİNİN CARI VƏZİYYƏTİ VƏ GEOLOJİ MƏDƏN GÖSTƏRİCİLƏRİ." *AZƏRBAYCAN RESPUBLİKASI TƏHSİL NAZİRLİYİ AZƏRBAYCAN DÖVLƏT NEFT VƏ SƏNAYE UNIVERSİTETİ*, 2015: 20-22.
9. Burns, Thomas G. "The Art and Science of Energy Forecasting." 2018.
10. Davis, John C. In *Statistics and Data Analysis in Geology 3rd Edition*, by John C. Davis, 487. Kansas Geological Survey, The University of Kansas, n.d.
11. F.V. Rahimov, A. Sh. Eminov, R. M. Huseynov. "Risk and Uncertainty Assesment while Estimtion of Reserves." *SPE - 189019*, 2017:p. 4.
12. *Hierarchical Clustering / Dendograms*. n.d. https://www.ncss.com/wp-content/themes/ncss/pdf/Procedures/NCSS/Hierarchical_Clustering-Dendograms.pdf.
13. "https://ncss-wpengine.netdna-ssl.com/wp-content/themes/ncss/pdf/Procedures/NCSS/Hierarchical_Clustering-Dendograms.pdf." https://ncss-wpengine.netdna-ssl.com/wp-content/themes/ncss/pdf/Procedures/NCSS/Hierarchical_Clustering-Dendograms.pdf. n.d. https://ncss-wpengine.netdna-ssl.com/wp-content/themes/ncss/pdf/Procedures/NCSS/Hierarchical_Clustering-Dendograms.pdf.
14. J. H. Schulze, SPE, J. N. Walker, SPE, M. K. Burkholder, SPE, Decision Frameworks, L.P. "Integrating the Subsurface and the Commercial: A New Look at Monte Carlo and Decision Tree Analysis." *SPE 162883*, 2012: p. 1-4.
15. *JMP Statistical Discovery* . n.d. <https://www.jmp.com/support/help/14-2/hierarchical-cluster.shtml>.
16. Joe H. Ward, Jr. *Journal of the Amarican Statistical Association* vol. 58 No. 301, March 1963: p. 238.

17. Leonid A. Buryakovsky, George V. Chilingar, Fred Aminzadeh. *Petroleum Geology of the South Caspian Basin*. 2001.
18. Mark Baker, Woodsiden. "Use of Cluster Analysis to improve Representative Model Selection: A Case Study ." *SPE - 176408 -MS*, 2015: 2.
19. Maureen Ani, Gbenga Aluyemi, Andrei Petrovski, Sina Rezaei-Gomari. "Reservoir Uncertainty Analysis: The Trends from Probability to Algorithms and Machine Learning ." *SPE* , 2016: 4.
20. Niels Jacob Haaning Andersen, Jeppe Brandstrup. *Monte Carlo Simulation in Crystal Ball 7.3* . AARHUS UNIVERSITY , 2008 .
21. ƏHMƏDOV ELVİN HACIQULU OĞLU. *NEFT YATAQLARININ QALIQ EHTİYATLARININ SƏMƏRƏLİ MƏNİMSƏNİLMƏ YOLLARININ GEOLOJİ ƏSASLANDIRILMASI VƏ RİSKLƏRİN QIYMƏTLƏNDİRİLMƏSİ (GÜNƏŞLİ VƏ NEFT DAŞLARI YATAQLARININ TİMSALINDA)* . BAKI : "NEFTQAZELMİTƏDQIQATLAYİHƏ" İNSTİTUTU , 2016.
22. Oracle. 2008. <https://www.oracle.com/technetwork/middleware/crystalball/overview/crystal-ball-131398.pdf>.
23. Oracle. 2008. <https://www.oracle.com/technetwork/middleware/crystalball/overview/crystal-ball-131398.pdf>.
24. Behrenbruch, G. J. Turner, A. R. Backhouse. "Probabilistic Hydrocarbon Reserves Estimation: A Novel Monte Carlo approach ." *SPE13982*, n.d.: p.3.
25. Parks, James M. "Cluster Analysis Applied to Multivariate Geologic Problems." *the Journal of Geology* vol. 74 no.5 part 2, 1966: p. 704-715.
26. Robert H., Caldwell, David I. Heather. "Characterizing Uncertainty In Oil and Gas Evaluations ." *SPE 68592*, 2001: p. 3.
27. SOCAR. "<http://www.socar.az/socar/en/company/about-socar/discover-socar>." <http://www.socar.az/socar/en/company/about-socar/discover-socar>. n.d. <http://www.socar.az/socar/en/company/about-socar/discover-socar>.
28. Stoian, E. "Fundamentals and Applications of the Monte Carlo Method ." 1965: p. 120-122.
29. Surek, Melahat Asli. *the Cluster Analysis of the Balakhany 8 reservoir unit with spectral gamma ray logs, Azeri-Chirag-Guneshli field, Offshore Azerbaijan*. Faculty of the Department of Earth and Atmospheric Sciences, University of Houston, December 2013.
30. V. J. Abdullayev, M.A. Huseynov, M.M. Ismailov, K.M.Nabiyev. "3D geological modelling of the Guneshli field ." n.d.: p. 76.
31. А. А. Фейзуллаев, В. Н. Лунина, Д. Р. Мирзоева. "Пространственные особенности изменения петрографических и коллекторских свойств пород продуктивной толщи (на примере месторождения Гюнешли, Южно-Каспийский бассейн)." *Институт геологии и геофизики НАН Азербайджана, Баку, Азербайджан*, 2018: p. 143.

